JNeurosci
THE JOURNAL OF NEUROSCIENCE

Research Articles: Neurobiology of Disease

MicroRNA-1224 splicing circularRNA-Filip1l in an Ago2- dependent manner regulates chronic inflammatory pain via targeting Ubr5

Zhiqiang Pan[1,2], Guo-Fang Li[1,2], Meng-Lan Sun[1,2], Ling Xie[1,2], Di Liu[1,2], Qi Zhang[1,2], Xiao-Xiao Yang[1,2], Sunhui Xia[1,2], Liu Xiaodan[1,2], Huimin Zhou[1,2], Zhou-Ya Xue[1,2], Ming Zhang[1,2], Ling-Yun Hao[1,2], Li-Jiao Zhu[1,2] and Jun-Li Cao[1,2,3]

[1]*Jiangsu Province Key Laboratory of Anesthesiology, Xuzhou Medical University, Xuzhou 221004, China.*
[2]*Jiangsu Province Key Laboratory of Anesthesia and Analgesia Application Technology, Xuzhou Medical University, Xuzhou 221004, China.*
[3]*Department of Anesthesiology, The Affiliated Hospital of Xuzhou Medical University, Xuzhou 221002, China.*

https://doi.org/10.1523/JNEUROSCI.1631-18.2018

Received: 29 June 2018

Revised: 10 December 2018

Accepted: 26 December 2018

Published: 16 January 2019

Author contributions: J.-L.C. and Z.P. designed research; J.-L.C. and Z.P. wrote the paper; Z.P., G.-F.L., M.S., L.X., D.L., Q.Z., X.-X.Y., S.X., X.L., H.Z., Z.-Y.X., M.Z., and L.H. performed research; Z.P. contributed unpublished reagents/analytic tools; Z.P., G.-F.L., M.S., L.H., and L.Z. analyzed data; Z.P. wrote the first draft of the paper.

Conflict of Interest: The authors declare no competing financial interests.

The study was supported by grants from the National Natural Science Foundation of China (81671096, 81271231 to Z. Pan, 31771161, 81720108013 to J.-L. Cao, 31500855 to L.-J. Zhu); Key project of the Natural Science Foundation of Jiangsu Education Department (15KJA320004 to Z. Pan); and the Project Funded by the Qing Lan Project, by the Six Talent Summit Project, by the 333 High-level Personnel Training Project.

Correspondence: Address correspondence: Jiangsu Province Key Laboratory of Anesthesiology, Xuzhou Medical University, 209 Tongshan Road, Xuzhou 221004, Jiangsu, PR China. Tel.: +86-516-83262686; E-mail to Dr. Zhiqiang Pan: zhiqiangp2002@aliyun.com; or to Dr. Jun-Li Cao: caojl0310@aliyun.com

Cite as: J. Neurosci 2019; 10.1523/JNEUROSCI.1631-18.2018

Title page

MicroRNA-1224 splicing circularRNA-Filip1l in an Ago2-dependent manner regulates chronic inflammatory pain via targeting Ubr5

Zhiqiang Pan,[1,2] * Guo-Fang Li,[1,2] * Meng-Lan Sun,[1,2] * Ling Xie,[1,2] Di Liu,[1,2] Qi Zhang,[1,2] Xiao-Xiao Yang,[1,2] Sunhui, Xia,[1,2] Xiaodan Liu,[1,2] Huimin Zhou,[1,2] Zhou-Ya Xue,[1,2] Ming Zhang,[1,2] Ling-Yun Hao,[1,2] Li-Jiao Zhu,[1,2] and Jun-Li Cao[1,2,3]

[1] Jiangsu Province Key Laboratory of Anesthesiology, Xuzhou Medical University, Xuzhou 221004, China.

[2]Jiangsu Province Key Laboratory of Anesthesia and Analgesia Application Technology, Xuzhou Medical University, Xuzhou 221004, China.

[3]Department of Anesthesiology, The Affiliated Hospital of Xuzhou Medical University, Xuzhou 221002, China.

Correspondence

Address correspondence: Jiangsu Province Key Laboratory of Anesthesiology, Xuzhou Medical University, 209 Tongshan Road, Xuzhou 221004, Jiangsu, PR

China. Tel.: +86-516-83262686; E-mail to Dr. Zhiqiang Pan: zhiqiangp2002@aliyun.com; or to Dr. Jun-Li Cao: caojl0310@aliyun.com

Acknowledgements

The study was supported by grants from the National Natural Science Foundation of China (81671096, 81271231 to Z. Pan, 31771161, 81720108013 to J.-L. Cao, 31500855 to L.-J. Zhu); Key project of the Natural Science Foundation of Jiangsu Education Department (15KJA320004 to Z. Pan); and the Project Funded by the Qing Lan Project, by the Six Talent Summit Project, by the 333 High-level Personnel Training Project.

Author contributions

Z.P, G.F.L, and M.L.S contributed equally to this work.

J.-L.C. and Z.P. designed research; Z.P., G.-F.L., M.-L.S., L.X., D.L., Q.Z., X.-X.Y., Z.-Y.X., M.Z., L.-Y.H., S.X., X. L., and H. Z. performed research; Z.P., G.-F.L., M.-L.S., H.-L.D., and L.-J.Z. analyzed data; J.-L.C. and Z.P. wrote the paper.

Words statistics

Number of words in Abstract: 225

Number of words in Introduction: 754

Number of words in Discussion: 1798

Figure statistics

Number of figures: 8

Running head

CircRNA-Filip1l regulates chronic pain

Competing Interests

The authors declare no competing interests.

Abstract

Dysfunctions of genes transcription and translation in the nociceptive pathways play the critical role in development and maintenance of chronic pain. Circular RNAs (circRNAs) are emerging as new players in regulation of gene expression, but whether and how circRNAs are involved in chronic pain remains elusive. We showed here that complete Freund's adjuvant (CFA)-induced chronic inflammation pain significantly increased circRNA-Filip1l (filamin A interacting protein 1-like) expression in spinal neurons of mice. Blockage of this increase attenuated CFA-induced nociceptive behaviors, and overexpression of spinal circRNA-Filip1l in naïve mice mimicked the nociceptive behaviors as evidenced by decreased thermal and mechanical nociceptive threshold. Furthermore, we found that mature circRNA-Filip1l expression was negatively regulated by miRNA-1224 via binding and splicing of precursor of circRNA-Filip1l (pre-circRNA-Filip1l) in the Argonaute-2 (Ago2)-dependent manner. Increase of spinal circRNA-Filip1l expression resulted from the decrease of miRNA-1224 expression under chronic inflammation pain state. MiRNA-1224 knockdown or Ago2 overexpression induced nociceptive behaviors in naïve mice, which was prevented by the knockdown of spinal circRNA-Filip1l. Finally, we demonstrated that an ubiquitin protein ligase E3 component n-recognin 5 (Ubr5), validated as a target of circRNA-Filip1l, plays a pivotal role in regulation of nociception by spinal

circRNA-Filip1l. These data suggest that miRNA-1224-mediated and Ago2-dependent modulation of spinal circRNA-Filip1l expression regulates nociception via targeting Ubr5, revealing a novel epigenetic mechanism of interaction between miRNA and circRNA in chronic inflammation pain.

Key words: circRNA; miRNA; Ubr5; nociception; spinal cord

106 **Significance Statement**

107

108 CircRNAs are emerging as new players in regulation of gene expression. Here,
109 we found that the increase of circRNA-Filip1l mediated by miRNA-1224 in
110 Ago2-dependent way in the spinal cord is involved in regulation of nociception via
111 targeting Ubr5. Our study reveals a novel epigenetic mechanism of interaction
112 between miRNA and circRNA in chronic inflammation pain.

113

114

115

116

117

118

119

120

121

122

123

124

125

126

Introduction

Emerging evidence has shown that malfunctions in regulation of gene expression mediated by epigenetic mechanisms play the critical role in development and maintenance of chronic pain induced by diverse causes (Imai et al., 2013; Ji et al., 2016; Pan et al., 2016; Jiang et al., 2017). The existing body of research suggests that the epigenetic regulation of gene expression by the widespread noncoding RNAs (ncRNAs) including miRNA and long ncRNA is involved in the process of inflammation or never injury-induced chronic pain (Zhao et al., 2013; Park et al., 2014; Jiang et al., 2016). However, the study of pain-related circular RNAs (circRNAs, a kind of ncRNAs) is still in its infancy.

CircRNAs, a large class of circularized RNAs in different species ranging from human and mouse to Drosophila and C. elegans, are characterized by a high stable structure and high tissue-specific expression (You et al., 2015; Chen and Schuman, 2016). Their expression is associated with such physiological and pathological processes as metabolism, cancer (Hansen et al., 2013a), atherosclerosis (Holdt et al., 2016), and myogenesis (Legnini et al., 2017). However, how they are causally linked to disease development remains elusive. Recent studies reveal that several circRNAs are specifically enriched in brain (Memczak et al., 2013; You et al., 2015; Chen and Schuman, 2016) or spinal cord (Zhou et al., 2017). Interestingly, these circRNAs are differentially expressed in

various brain regions or in neuronal subcellular fraction, and notably involved in brain development, neuronal differentiation and synaptic plasticity (Rybak-Wolf et al., 2015). These characteristics imply their potential involvement in the pathogenesis of a variety of central nervous system (CNS) diseases. Accumulating evidence indicates that their aberrant expression or functional consequences contribute to the initiation, development, maintenance of various neurological disorders such as epilepsy, Parkinson's disease (PD) (Kumar et al., 2018), Alzheimer's disease (AD) (Shao and Chen, 2016), and pain (Cao et al., 2017; Zhou et al., 2017). The expression profiling shows that spared nerve injury (SNI) leads to 68 up-regulation and 120 down-regulation of circRNAs in rat spinal cord, furthermore, *in vitro* luciferase assay shows that circ-0006928 regulates chronic pain by targeting miRNA-184 (Zhou et al., 2017). Despite the fact in favor of circRNA's relevant potential therapeutic tool for CNS-related diseases, the role of circRNAs in the aberrant gene expression has not been explored in chronic pain. CircRNA-Filip1l, named as circ-0000691 in circbase data (Memczak et al., 2013), is firstly found in mouse cerebella tissue (Glazar et al., 2014), and its expression is further confirmed in mammalian brain (Rybak-Wolf et al., 2015). Our circRNA profiling showed that circRNA-Filip1l was significantly increased in the spinal cord of complete Freund's adjuvant (CFA)-induced chronic inflammatory pain mice. However, it is unclear whether and how circRNA-Filip1l participates in the process of chronic pain.

Recently, a strong link between miRNA dysregulation and chronic pain has been established (Descalzi et al., 2015). Manipulation of miRNA expression in pain pathways from primary afferent nociceptors, DRG, spinal cord, and brain associated with pain perception prevents or reverses persistent inflammatory, neuropathic, and cancer pain behavior by post-transcription in cytoplasma (Park et al., 2014; Jiang et al., 2016; Gandla et al., 2017; Zhang et al., 2017). Growing findings suggest that the majority of miRNAs exist in both nucleus and cytoplasma, and some are preferentially enriched in the nucleus (Roberts, 2014; Rasko and Wong, 2017). Furthermore, the assembled Ago2-miRNA complexes are required for modulation of splicing or transcription of mRNA or circRNA through miRNA binding in nucleus. MiRNA-671 directs the cleavage of a circular antisense transcript of cerebellar degeneration-related protein 1 (CDR1) in Ago2-dependent manner in nucleus, resulting in the down-regulation of circular antisense, suggesting a crucial function of miRNA-mediated Ago2 cleavage in the modulation of circRNA expression (Hansen et al., 2011). MiRNA-1224 is relatively conserved in mammal cells, and is abundantly expressed in CNS tissues such as brain cerebral (Hunsberger et al., 2012), hippocampus and the marginal division (Shu et al., 2013). In HEK293T cell, up-regulation of miRNA-1224 with mimics silences the expression of LRRK2 and α-synuclein associated with PD (Sibley et al., 2012), supporting the potential regulatory role of miRNA-1224 in CNS

diseases-related genes. However, it is still unknown whether miRNA-1224 is involved in chronic pain.

In the current work, we found the increase of circRNA-Filip1l and decrease of miRNA-1224 in mouse spinal cords in a CFA-induced inflammation pain model. Moreover, miRNA-1224 is predictively bound to the splice junction of precursor-circRNA-Filip1l (pre-circRNA-Filip1l). Thus, we hypothesized that the circRNA-Filip1l cleaved by miRNA-1224 in an Ago2-dependent manner contributes to the development and maintenance of chronic inflammatory pain.

Materials and Methods

Animals, pain model, and behavior testing. All animal procedures were approved by the animal care committee of Xuzhou Medical University (Xuzhou, China). All efforts were made to minimize animal suffering and to reduce the number of animals used. Mice were housed at 23 ± 3 °C with humidity ranges between 25 and 45%, and maintained on a 12:12 light / dark cycle (06:00 to 18:00 h) with access to food and water *ad libitum*. Adult male Shanghai populations of Kunming mice (20 - 25 g) were used in this study. The animals were randomized to either a control or an experimental group. Chronic inflammatory pain was induced by subcutaneous administration of CFA (40μl; F5881; Sigma-Aldrich, USA) into the plantar surface of the left hind paw. A 0.9% saline solution was used as a control for CFA. Unilateral sciatic nerve chronic constrictive injury (CCI) model was performed as described (Pan et al., 2014). Mice were anesthetized with inhalation anesthesia by isoflurane in O_2. Under the anesthesia condition: blunt dissection was made into the skin overlying the area between the gluteus and biceps femoris muscles, and the common left sciatic nerve of the hind paw was exposed at the mid-thigh level. Approximately 7mm of nerve was freed, proximal to the sciatic trifurcation, and three loose ligatures (about 1 mm space) of 7–0 silk thread were placed around the sciatic nerve, until a brief twitch was observed. Sham-operative groups underwent identical procedures but no ligation of the respective nerve.

After surgery, all mice were maintained in a warm electric blanket with stable temperature until they recovered from anesthesia.

Paw withdrawal latency to a thermal stimulus and paw withdrawal thresholds to a mechanical stimulus were used to measure hyperalgesia and allodynia as described previously (Pan et al., 2017). Before nociceptive behavior testing, mice were acclimatized to the environment for 1h. Thermal hyperalgesia was assessed with an analgesia meter (IITC Model 336 Analgesia Meter, Series 8; IITC Life Science Inc.; Woodland Hills, CA, USA) by focusing a beam of light on the plantar surface of the hind paw to generate heat. The time required for the stimulus to elicit withdraw of the hind paw was recorded. The radiant heat intensity was adjusted to obtain basal paw withdrawal latency of 11 to 14s. An automatic 20s cutoff was used to prevent tissue damage. Thermal stimuli were delivered three times to each hind paw at 5-min intervals. Mechanical allodynia was assessed with the use of Von Frey filaments (Stoelting Inc., Chicago, IL, USA), starting with a 0.16g and ending with a 6.0g filament. The filaments were presented five times respectively at 5 min intervals, in ascending order of strength, perpendicular to the plantar surface with sufficient force to cause slight bending against the paw. A brisk withdrawal or flinching of the paw was considered a positive response. All behavioral tests were performed in a double blind trial fashion in this study.

Locomotors function. Three reflex tests were carried out as follows. To test the grasping reflex, climbing tests were carried out according to previously described procedures (Zhang et al., 2014). A 0.5mm diameter metal wire mesh with a 5mm wide grid was placed vertically 30cm above the table. Each mouse started at the bottom of the mesh with its head facing downward. After the mouse was released, the time required for it to climb all the way to the top was recorded. A maximum time of 60s was applied for animals that could not successfully complete this task. Two sessions were performed for each mouse with a 30min interval, and the shorter time was recorded. To test the placing reflex (Tao et al., 2003), we held the mouse with the hind limbs slightly lower than the forelimbs and brought the dorsal surfaces of the hind paws into contact with the edge of a table. The experimenter recorded whether the hind paws were placed on the table surface reflexively. To test the righting reflex (Tao et al., 2003), we placed the mouse on its back on a flat surface; the experimenter noted whether it immediately assumed the normal upright position. Scores for placing, grasping, and righting reflexes were based on the counts of each normal reflex exhibited in five trials.

Spinal tissue collection. Mice were anesthetized with 10% chloral hydrate, and the spinal cord within the lumbar segments (L3-L5) was removed rapidly. The dorsal spinal cord ipsilateral to CFA was separated and snap-frozen in liquid nitrogen, and stored at −80°C.

CircRNA-microarray. Total RNA from each of 6 samples was quantified using the NanoDrop ND-2000. The sample preparation and microarray hybridization were performed according to Arraystar Mouse circRNA's standard protocols (Arraystar Inc.). Briefly, total RNA from each sample was firstly treated with Rnase R (Epicentre, Inc.) to obtain circRNA through removing linear RNAs. Then, each sample was amplified and transcribed into fluorescent cRNA utilizing a random priming method (Arraystar Super RNA Labeling Kit; Arraystar). The labeled cRNAs were purified by RNeasy Mini Kit (Qiagen). The concentration and specific activity of the labeled cRNAs (pmol Cy3/μg cRNA) were measured by NanoDrop ND-2000. 1μg of each labeled cRNA was fragmented by adding 5μl 10 × Blocking Agent and 1μl of 25 × Fragmentation buffer, then heated the mixture at 60 °C for 30min, finally 25μl 2 × Hybridization buffer was added to dilute the labeled cRNA. 50μl of hybridization solution was dispensed into the gasket slide and assembled to the circRNA expression microarray slide (6 x 7K, Arraystar). The slides were incubated for 17h at 65°C in an Agilent Hybridization Oven. After having washed the slides, the arrays were scanned by the Axon GenePix 4000B microarray scanner. Scanned images were then imported into GenePix Pro 6.0 software (Axon) for grid alignment and data extraction. Quantile normalization and subsequent data processing was performed using the R software package. After quantile normalization of the raw data, low intensity filtering was performed, and the circRNAs that at least 1 out of 3 samples have flag "expressed" (greater than

2 times background standard deviation) were retained for further analyses. Differentially expressed circRNAs with statistical significance between two groups were identified through Volcano Plot filtering. The statistical significance of the difference was conveniently estimated by t-test. CircRNAs having fold changes≥2 and p-values≤0.05 were selected as the significantly differentially expressed.

RNA, circRNA, miRNA, and RT-qPCR. Total RNA was isolated with a Trizol reagent (15596-026; Invitrogen, USA) to generate cDNA templates by reverse transcription reactions with oligo (dT) for Ago2, and Filip1l, or with random primers for circRNA-Filip1l, and pre-circRNA-Filip1l, and reverse transcriptase M-MLV (2641A; Takara Bio, Japan) at 42°C for 60 min. cDNA products were used as templates to detect gene mRNA (Ago2: F: 5'-CGTCCTTCCCACTACCACG-3', R: 5'-CCAGAGGTATGGCTTCCTTCA-3'；Ubr5: F: 5'-TGAGGTTTCTACGATCTGTG GC-3', R: 5'-AAACACACGTTTGCATTTTCCA-3'; Filip1l: F: 5'-CACA GGGTAAA CTAGCCCTTG-3'; R: 5'-TGGCGATTTTGACTGTCCTCA-3' and pre-circRNA-Filip1l: F: 5'-CTCTGGTCACCTGGTGGGAT-3', R: 5'-TGGGTAGAGGCAATTTG GCA-3') or circRNA expression (circRNA-Filip1l: F: 5'-AGGCCTCGGGATCCCAC CTC-3', R: 5'-TCCAGTCCGCCGAGGGCGC-3'；circRNA-014740：F: 5'-AGACA TTGATGACTGCTTATGC-3', R: 5'-CATAGCCCTGGTCACAACT-3'; circRNA-16648：F: 5'-TTGGAGCTGCTGGCCCATCC-3', R：5'-GCATTGTTGGTCCAACC GGGTCT-3'; circRNA-005786: F: 5'-CTTGGCCTCTTCCTCCTTTT-3', R: 5'-TGG

GCCTCAGGAAGTAGAGA-3') via RT-qPCR with SYBR Premix ExTaqII (RR820A; Takara Bio) according to the manufacturer's instructions. miRNA was reversely transcribed at 16°C for 30min, and 37°C for 30min using specific primer 1224RT (5'-TTAACTGGATACGAAGGGTCCGAACACCGGTCGTATCCAGTTAActccacc-3'). RT-qPCR was performed using primer pairs 1224F: 5'-TGCGGGTGAGGAC TGGGGAG-3' and 1224R: 5'-TACGAAGGGTCCGAACAC-3'. RNase R treatment was performed as follows: 5 μg of total RNA was diluted in 20μl of water with 4U RNase R/μg unless differently stated and 2μl of enzyme buffer (Epicenter), then incubated 15min at 37°C and purified by phenol chloroform extraction. Reactions were performed in triplicate. Gapdh (GF, 5'-GGTGAAGGTCGGTGTGAACG-3'; GR, 5'-CTCGCTCCTGGAAGATGGTG-3') was used as an internal control of Ago2, Ubr5, Filip1l and and pre- circRNA-Filip1l. U6 snRNA (6F, 5'-CTCGCTTCG GCAGCACATATACT-3'; 6R, 5'-ACGCTTCACGAATTTGCGTGTC-3') was used as an internal control of miRNA-1224 and circRNA-Filip1l. The expression levels of the target genes were quantified relative to Gapdh or U6 snRNA expression (cycle threshold, CT) using the $2^{-\Delta\Delta CT}$ methods. Any value among triplicates that had a marked difference (≥1.00) compared with the average of the other two was omitted.

Spinal neuron culture. The primary culture of spinal neurons was carried out according to the previous described (Hugel and Schlichter, 2000). Briefly, after

decapitation of 3- to 4-d-old mice under deep anesthesia, a laminectomy was performed, and the third dorsal of the spinal cord was cut with a razor blade. The tissue fragments were digested enzymatically for 45min at 37°C with papain (20 U/ml, Sigma, St. Louis, MO) in oxygenated divalent-free Earle's balanced salt solution (EBSS, Life Technologies, Gaithersburg, MD). The enzymatic digestion was stopped by adding 3ml EBSS containing bovine serum albumin (1 mg/ml; Sigma), trypsin inhibitor (10 mg/ml; Sigma), and DNase (0.01%; Sigma), and a mechanical dissociation were performed with a 1ml plastic pipette. The homogenate was deposited on top of 4ml of a solution of composition similar to that described above, except that the concentration of bovine serum albumin was increased to 10 mg/ml. After centrifugation (5min at 500rpm), the supernatant was removed and replaced with 5ml of culture medium the composition of which was the following: MEM-α (Life Technologies), fetal calf serum (5% vol/vol; Life Technologies), heat-inactivated horse serum (5% vol/vol; Life Technologies), penicillin and streptomycin (50 IU/ml for each; Life Technologies), transferrin (10 mg/ml; Sigma), insulin (5 mg/ml; Sigma), putrescine (100nM; Sigma), and progesterone (20nM; Sigma). After trituration with a fire-polished Pasteur pipette, the cells were plated on 35mm collagen-coated plastic culture dishes in the central compartment, which was delimited by a small (internal diameter 15mm) circular glass ring. This ring was glued onto the bottom of the dish with paraffin wax and could easily be removed before electrophysiological experiments.

Cultures were maintained in a water-saturated atmosphere (95% air, 5% CO_2) at 37°C until use (10–15 d). Two days after the cells were seeded; cytosine arabinoside (10μM) was added to the culture medium for 24h to reduce glial proliferation.

Spinal astrocytes- and mircoglia cultures.

The isolation of spinal astrocytes and mircoglia cells was carried out according to the previous described (Monif et al., 2016) with few modifications. The third dorsal of spinal cord from 3- to 4-d-old mice was cut, the tissue fragments were digested enzymatically for 45 min at 37°C with trypsin (0.25 %, Gibco), and stopped by adding equal volume DMEM with 10% FBS, then centrifuged at 1000g for 30s, removed the supernatant, washed three times with DMEM with 10% FBS, centrifuged at 1000g for 30s each time. The mixed cells were suspended by the use of DMEM with 20% FBS, and filtered with 200 mesh sieve. The suspended cells were plated into 75 cm^2 plate. After 30min, transfered the medium to the 75 cm^2 flsak, cultured at 37°C for 7-10 days. To harvest the astrocytes, the flasks of mixed glial cells were shaken at 220 rpm at 37°C overnight, discarded the supernatant, the left was the astrocytes, and then added DMEM with 10% FBS, and continued to culture at 37°C till to the cellular astrocyte density required. To harvest microglial cells, the flasks of mixed glial cells were shaken at 150 rpm at 37°C for 4h, collected the supernatant containing the microglial cells to the new

plates, and continued to perform the culture at 37°C, till to the density of microglial cells required

Cellular fraction and RNA isolation. PARIS™ Kit (Life Technologies, #AM1921) was used to separately isolate nuclear and cytoplasmic RNA from cultured mouse spinal neurons, following the manufacturer instructions.

Immunofluorescence and fluorescence in situ hybridization. The procedure was performed as described in a previous study (Pan et al., 2014). In brief, spinal cords were rapidly dissected from perfused mice and fixed with 4% PFA, then cryoprotected in 30% sucrose. For fluorescence *in situ* hybridization (FISH) in cultured cells, digoxin labeled circRNA-Filip1l probe (Dig-Filip1l, 5'-Dig-CGCCGG GGAGGTGGGATCCCGA-Dig-3') or miRNA-1224 probe (Dig-1224, 5'-Dig-CTCC ACCTCCCCAGTCCTCAC-Dig-3') was hybridize to spinal slices as instructed in the FISH kit (Guangzhou Exon), and incubated with then fluorescent-conjugated secondary anti-digoxin, and then after PBS wash 3 times FISH sections were incubated with NeuN antibody (MAB377, Millipore), finally after PBS wash 3 times incubated with fluorescent-conjugated secondary antibody (Alexa-594, Cell Signaling Technology). After the sections were rinsed in 0.01M PBS, coverslips were applied.

Northern blot. Northern blot was performed according to the previous described (Legnini et al., 2017) with modified. Briefly, 10µg RNA was denatured with one volume of glyoxal loading dye (Ambion) at 50°C for 30 min and loaded on 1.2% agarose gel. Electrophoresis was carried out for 2.5h at 60V. RNA was transferred on Hybond N^+ membrane (GE Healthcare) by capillarity overnight in 10×SSC. Transferred RNA was cross-linked with UV at 1200×100 mJ/cm^2 and the membrane was washed in 50mM Tris pH 8.0 at 45°C for 20min. Prehybridization and hybridization were performed in Northern Max buffer (Ambion) at 68°C for 30min and overnight, respectively. 500ng of DIG-labeled probe in 10mL were used for hybridization. The membrane was then washed with 2×SSC 0.1% SDS twice 30min, then once 30min and once 1h with 0.2×SSC 0.1% SDS at hybridization temperature. The membrane was the processed for DIG detection (hybridization with anti-DIG antibody, washing and luminescence detection) with the DIG luminescence detection kit (Roche), according to the manufacturer instructions. DIG-labeled probes were produced by in vitro transcription with DIG-RNA labeling kit (11175025910, Roche) of PCR templates produced with the primers DFilip1IF (5'-AGGCCTCGGGATCCCACCTC-3') and DT7-Filip1IR (5'-TA ATACGACTCACTATAGGTCCAGTCCGCCGAGGGCGC-3'), used with mouse cDNAs. circRNA transcription with T7 RNA polymerase (Promega) was carried out at 37°C for 2h, then purified with Micro Bio-Spin 30 Chromatography Column (732-6223, Bio-Rad).

Synthetic anti-circRNA and circRNA mimics. The anti-circRNA-Filip1l mimics and linear circRNA-Filip1l were obtained by *in vitro* transcription from a PCR-generated template, respectively with anti-circRNA-Filip1l primer pair (DFilip1lF and DT7-Filip1lR) and linear circRNA-Filip1l primer pair (DT7- Filip1lF, 5'-TAATACGACTCACTATAGGGCTCCCCGGCGCGGCGGG-3'/Filip1lR, 5'-GAG GTGGGATCCCGAGGCCT-3' (using mouse cDNA as PCR template) in presence of T7 polymerase (Promega) following the manufacturer's instructions, and purified with Micro Bio-Spin 30 Chromatography Column (732-6223, Bio-Rad) after DNase treatment. circRNA-Filip1l was synthesized using linear circRNA-Filip1l according to the previous described (Legnini et al., 2017). A phosphate group was then attached to the 5'-OH using ATP and T4 Polynucleotide kinase (BioLabs); the linear transcript carrying no 5'-phosphate and 3'-OH ends was subjected to Ethanol precipitation in presence of 10mg of glycogen (Roche). Ligase reaction was carried out in a final volume of 100µl, incubating the linear transcript at 95°C for 2min followed by 5min at 75°C in presence of 10% DMSO. T4 RNA Ligase (BioLabs), 1×T4 RNA Ligase Buffer, 10mM ATP and RNase inhibitor were then added and the reaction was carried out at 16°C for 16h. The circularized RNA product was separated and purified from the linear transcript by polyacrylamide gel electrophoresis. Thirty nanograms of both circular and linear transcripts were subjected to RNase R treatment followed by qRT-PCR to assess the circularity of the gel-purified RNA molecules.

Plasmid construction. All constructs were produced by the use of standard molecular methods and confirmed by DNA sequencing. To construct circRNA-Filip1l, miRNA-1224, and Ago2 overexpression vectors (OE): one insert prepared by PCR using primer pairs [circRNA-Filip1l OE: PWFilpF, 5'-ACGCTC GAGAGTGGCCCACTAGGCACTC-3' (XhoI)/PWFilpR, 5'-GGCGTTTAAACAAAC AATAAGTCTGGGAGAG-3' (PmeI); miRNA-1224 OE: PW1224F, 5'-CGGGATCC GAGCCCATATCTCCTACTGG-3' (BamhI)/PW1224R, 5'-AATACGCGTTCGACA CAGGCGTTCTTGAG-3' (MluI); and Ago2 OE: PW-Ago2F, 5'-AATGGATCCATG TACTCGGGAGCCGGCCC-3' (BamHI)/PW-Ago2R, 5'-AATACGCGTTCAAGCAA AGTACATGGTGCGC-3' (MluI)] and PWPXLvector were digested by corresponding double restriction endonucleases (NEB), and then ligated with T4 ligase. To construct circRNA-Filip1l overexpression vectors in DNA3.1 plasmid: one insert from PCR with PCR pair [5'-ACGAAGCTTAGCCTGAGTTTGCCATCT TG-3' (HindIII) and 5'-ACGCTCGAGTCAAAGAAACTAACGGCAAC-3' (XhoI)] and the digested cDNA3.1 vector, and then ligated with T4 ligase. To construct circRNA-Filip1l, miRNA-1224 and Ubr5 knockdown vector (KD), LV-anti-Filip1lF [5'-P-CGCGCCCACCTCCCTCCCCGGCGCGGCGGGCGAGACGGGCCGGTG G-3' (MluI)] and LV-anti-Filip1lR [5'-P-CGCCACCGGCCCGTCTCGCCCGCCG CGCCGGGGAGGGAGGTGGG-3' (ClaI)], or PLV-1224F [5'-P-CGCGGTGAGGA CACCGAGGTGGAGtagcGTGAGGACACCGAGGTGGAG-3' (MluI)] and PLV-1224R [5'-P-CGCTCCACCTCGGTGTCCTCACgctaCTCCACCTCGGTGTCCTC

AC-3'(ClaI)] or PLV-Ubr5F [5'-P-CGCGGAATGTACTGGAGCAGGCTACTATTCG AAAATAGTAGCCTGCTCCAGTACATTC-3' (MluI)] and PLV-Ubr5R [5'-P-CGGA ATGTACTGGAGCAGGCTACTATTTTCGAATAGTAGCCTGCTCCAGTACATTCC G-3' (ClaI)] was annealed and ligated to the digested PLVTHM vector, respectively.

Lentivirus production and verification. The constructed core plasmid (16μg) and two envelope plasmids, PSPAX2 (12μg) and PMD2G (4.8μg), were co-transfected into HEK293T cells in a 6-well plate according to manufacturer instructions of Lipofectamine 2000 (11668-027, Invitrogen). The supernatant was collected at 48h after transfection, and concentrated by using a Centricon Plus-70 filter unit (UFC910096, Millipore). Lentivirus with titers 10^8 TU/ml was used in the experiment. The assays of lentivirus in vitro and in vivo infection were performed according to previous study (Pan et al., 2014). Briefly, 20μl lentivirus and 1.5μl polybrene (1.4 μg/μl; H9268, Sigma-Aldrich) were added in a 24-well plate containing 1×10^5 HEK293T cells and DMEM without FBS; after 24h, the transfection medium was replaced with 500μl fresh complete medium containing 10% FBS; cells were collected at 48h after culture.

For *in vivo* verification of lentivirus, daily intrathecal injections of lentivirus or vector (1μl) were performed for 2 consecutive days in naïve or pain mice, then

collected samples day 3 after the first injection. Otherwise please saw the specified injection time points detailed in corresponded figure legend.

SiRNA, mimics, inhibitor, and lentivirus delivery. Injections were performed by holding the mouse firmly by the pelvic girdle and inserting a 30-gauge needle attached to a 25-μl microsyringe between L5 and L6 vertebrae. Proper insertion of the needle into the subarachnoid space was verified by a slight flick of the tail after a sudden advancement of the needle. Injections of 5μl of 20μM siRNAs, mimics and inhibitor for circRNA-Filip1l (5'-GCGCCGGGGAGGUGGAGCACGAGC-3'), Ago2 (sense: 5'-GCGCCGGGGAGGCGGAGCCACGAGCTT-3', antisense: 5'-GCTCGTGGCTCCGCCTCCCCGGCGCTT-3'), Ubr5 (sense: 5'-GAAUGUACUGGAGCAGGCUACUATT-3', antisense: 5'-UAGUAGCCUGCUCCAGUACAUUCTT-3'), or 1μl Lentivirus were performed daily for 3 days in a double blind trial fashion. Knockdown via Ago2-siRNA, ubr5-siRNA, PLV-Ubr5 was confirmed with RT-qPCR from samples of the ipsilateral dorsal spinal cord taken 72h after the last injection. Animals receiving intrathecal injections of scrambled siRNA or an empty vector were used as control groups.

Construction of reporter vector. The defined region of Ubr5 promoter was amplified from mouse genomic DNA using primer pairs (G6-U5F, 5'-ACGCTCGAGCAGGCTGCGAGACGGAGAAAC-3' and G6-U5R, 5'-AATAAGCTTCAGCGGG

TGGACCACGAAAT-3'), and cloned into pGL6 plasmid (Beyotime) via XhoI and HindIII digestion. Empty pGL6 vector was used as control plasmid. To construct the psiCK-wt-Filip1l or psiCK-mut-Filip1l reporter vector, psiCK-wtF [5'-P-TCGAGTCCTAACGCGTACGCTCGTGCTCCACCTCCCCGGCGCGGCGGGCGAGACGGGC-3' (XhoI)] (Underlined presents the reverse complementary fragment in pre-circRNA-Filip1l to miRNA-1224) and psiCK-wtR [5'-P-GGCCGCCCGTCTCGCCCGCCGCGCCGGGGAGGTGGAGCACGAGCGTACGCGTTAGGAC-3' (NotI)], or psiCK-mutF [5'-P-TCGAGTCCTAACGCGTACGCTCGTGCTAATCAGTTCCGGCGCGGCGGGCGAGACGGGC-3' (XhoI)] and psiCK-mutR [5'-P-GGCCGCCCGTCTCGCCCGCCGCGCCGGAACTGATTAGCACGAGCGTACGCGTTAGGAC-3' (NotI)], were annealed and ligated to the digested psiCHECK2 vector, respectively.

Single cell RT-PCR. Single-cell RT-PCR for spinal neurons was performed as described previously with few modifications (Jiang et al., 2016). Briefly, the contents of dissociated spinal neurons from CFA mice were harvested into patch pipettes with tip, placed gently into reaction tubes with Dnase I at 37°C for 30min, and heated to 80°C for 5min to remove genomic DNA. Reverse transcriptase (SuperScript III Platinum; Invitrogen) and specific reverse outer primer or 1224-RT was added, the sample was incubated at 50°C for 50min, and the reaction was terminated at 70°C for 15min. The cDNA products were used in gene-specific

nested PCR. The first-round PCR was performed with the outer primer pair (outF and outR) in the FastStart universal SYBR green master kit (Roche, Switzerland). PCR conditions were as follows: 1 cycle of 3min at 94°C; 5 cycles of 15s at 95°C and 5min at 56°C, 30s at 72°C ; then 20 cycles of 15s at 95°C and 15s at 60°C, 30s at 72°C,and 1 cycle of 10min at 72°C. The second round of PCR was carried out using 0.5μl of the first PCR product as the template and with inner PCR primers (inF and inR). The amplification: 1 cycle of 3 min at 94°C; 35 cycles of 15s at 95°C and 15s at 60°C, 30s at 72°C, and 1 cycle of 3min at 72°C. A negative control was obtained from pipettes that were submerged in the bath solution only. Gapdh was used as the reference gene. The primers are shown as the following：circRNA-Filip1l: outF/inF, 5'-ACTGGAGAGGCCTCGGGATC-3'; outR, 5'-CGCCGAGGGCGCACCACC-3'; inR, 5'-CGCACCACCGGCCCGTGGC-3'. miRNA-1224: RT, and outF/outR same as 1224RT, and 1224F/1224R above, respectively; inF, 5'-GGGTGAGGACTGGGGAG-3'; inR, 5'-AAGGGTCCGAACACCGG-3'. Ago2: outF, 5'-AGTTTGACTTCTACCTGTGCA-3'; outR, 5'-TGTGTCCTGGTGGACCTGGA-3'. inF/inR same as Ago2 F/R above. Ubr5: outF, 5'-AGAAGCAATTGCCGTGACAAT-3', outR, 5'-TGCTTGCCTGATCTGATGAC-3'. inF, 5'-TGAGGTTTCTACGATCTGTGGC-3'; inR, 5'-AAACACACGTTTGCATTTTCCA-3'. NeuN: outF, 5'-AGACAGACAACCAGCAACTC-3'; outR, 5'-CTGTTCCTACCACAGGGTTTAG-3'. inF, 5'-ACGATCGTAGAGGGACG-3'; inR, 5'-TTGGCATATGGGTTCCCAGG-3'. Gapdh: outF, 5'-AGGTTCATCAGGTAAACTCAG-3'; outR, 5'-ACCAGTAGAC

TCCACGACAT-3'. inF, ACCAGGGCTGCCATTTGCA; inR, 5'-CTCGCTCCTGGA AGATGGTG-3'.

Luciferase reporter assay. HEK293T cells were cultured in DMEM with10% FBS. HEK293T cells were seeded at 1×10^5 cells per 24-well. Identification of target was performed by transfecting reporter plasmids (50ng) and DNA3.1-Filip1l (80ng) or Lenti-Ago2 vector (80ng), or miRNA-1224 mimics (80ng) or inhibitor (50ng) into HEK293T cells using Lipofectamine 2000 (11668-027, Invitrogen) in a 24-well plate. Cell lysates were prepared and subjected to luciferase assays using the Double luciferase reporter kit (E1910, Promega) at 48h after transfection according to the manufacturer's instruction. pRL-TK plasmid was used as an internal control (Promega).

RNA-binding protein immunoprecipitation (RPIP). Immunoprecipitations were performed using Magna RIP™RNA-Binding Protein Immunoprecipitation Kit (17-700, Millipore). Briefly, spinal cord was harvested and placed in ice-cold PBS, then homogenized and centrifuged 1500rpm for 5min at 4°C, obtained the supernatant. Added 50μl of magnetic beads and ~5μg of the antibody of Ago2 (ab186733, Abcam) in each tube, incubated with rotation for 30min at room temperature. Then, re-suspend the mixture by RIP immunoprecipitation buffer and added the tissue supernatant, incubated with rotation for overnight at 4°C and

565 pull down the RNA on the magnetic rack. Finally, digested the protein with
566 proteinase K and extracted RNA for PT-qPCR.
567
568 *RNA-RNA in vivo precipitation (RRIP).* According to the previously described (Su
569 et al., 2015) with modification, biotin-labeled miRNA-1224 probe (Bio-1224, 5'-CT
570 CCACCTCCCCAGTCCTCAC-Bio-3') was used to perform the RRIP experiment
571 assay. Spinal cord was harvested 24h after intrathecal injection of Bio-1224 (5μl,
572 20μM) and fixed by 2.5% formaldehyde for 10min, lysed and sonicated. After
573 centrifugation, 50μl of the supernatant was retained as input and the remaining
574 part was incubated with Dynabeads M-280 Streptavidin (11205D, Thermo Fisher
575 Scientific) mixture over night at 4℃. Next day, beads-probes-RNAs mixture was
576 washed and incubated with 200μl lysis buffer and proteinase K to reverse the
577 formaldehyde crosslinking. Finally, the mixture was added with TRizol for RNA
578 extraction and detection.
579
580 *Western blot analysis.* Proteins (20 to 50 μg/sample) were separated by 10% SDS
581 polyacrylamide gel electrophoresis and transferred onto nitrocellulose
582 membranes, and incubated simultaneously at 4°C overnight in the corresponding
583 antibodies against: Ago2 (1:500, ab186733; Abcam), Ubr5 (1:1000, 65344; Cell
584 signaling), or control Tubulin β polyclonal antibody (1:5000; AP0064; bioworld).
585 The membranes were then washed twice in tris-buffered saline with Tween-20 at

586 room temperature for 10min, incubated with HRP-labeled Goat Anti-Rabbit IgG
587 (1:1000; A0208; Beyotime) at room temperature for 1h, and washed twice again in
588 Tris-buffered saline with Tween-20 at room temperature for 10min. The immune
589 complexes were detected with an NBT/BCIP (nitro blue tetrazolium/
590 5-bromo-4-chloro-3-indolyl-phosphate) assay kit (72091; Sigma-Aldrich). Band
591 analyses were performed in ImageJ software, with the intensities of the target
592 signals normalized to those of β-actin for statistical analyses.
593
594 *Statistical analysis.* All **d**ata were presented as mean values ± SEM. The data
595 were statistically analyzed with a one-way or two-way ANOVA or paired or
596 unpaired Student's t test. When ANOVA showed a significant difference, pairwise
597 comparisons between means were tested by the post hoc Tukey method.
598 Statistical analyses were performed with Prism (GraphPad 5.00, USA). $p < 0.05$
599 was considered statistically significance in all analyses.
600
601
602
603
604
605
606

Results

Profiling of spinal circRNAs in CFA-induced chronic inflammatory pain

The abundance of circRNAs in the CNS suggests its potential roles in dynamic regulation of structure and function of the CNS (Shao and Chen, 2016). To identify spinal circRNAs involved in chronic inflammation pain, we analyzed the circRNA expression profiling from ipsilateral dorsal spinal cord of chronic inflammation pain mice and control mice. 16 up-regulated and 34 down-regulated circRNAs with > 2.0 fold difference were obtained from 1099 candidates (Fig. 1*A*). CircRNA-005252 with most significant difference, and other three randomly selected circRNAs, including 1 up-regulated and 2 down-regulated in microarray analysis, were further confirmed by qRT-PCR (Fig. 1*B*). CircRNA-005252 (namely circRNA-Filip1l or mmu_circ_0000691 in cirbase database (Memczak et al., 2013)) --- was up-regulated by 2.8 fold. The further analysis showed that circRNA-Filip1l was located on Chr16: 57391624 - 57391694 (+), and back spliced by intron 1 of Filip1l, the distinct product of the expected size was amplified using outward-facing primers and confirmed by Sanger sequencing (Fig. 1*C*). We then investigated the stability and localization of circRNA-Filip1l in spinal cells. Resistance to digestion with RNase R exonuclease showed that circRNA-Filip1l was resistant to RNase R digestion, whereas linear Filip1l mRNA was easily degraded; further confirming that circRNA-Filip1l specie was circular in form (Fig.

628 1*D*). Northern blot assay verified the size of circRNA-Filip1l expected in spinal
629 RNA of adult mouse (Fig. 1*E*). Furthermore, to clarify the distribution of
630 circRNA-Filip1l in nucleus and cytoplasma, we separated the nucleus RNA and
631 cytoplasmic RNA from *in vitro* cultured spinal neurons to detect the content of
632 circRNA-Filip1l. RT-qPCR showed that the circRNA-Filip1l was localized in both
633 nucleus and cytoplasma fraction (Fig. 1*F*). Fluorescence *in situ* hybridization
634 further confirmed its localization in nucleus and cytoplasma of spinal neurons (Fig.
635 1*G*). These findings suggest that circRNA-Filip1l is an abundant and stable
636 circular noncoding RNA expressed in spinal cord of mice.
637
638 **Expression patterns of spinal circRNA-Filip1l underlying chronic pain**
639 To uncover a temporal expression pattern of circRNA-Filip1l in spinal cord in
640 chronic inflammation pain mice, we detected expression level of circRNA-Filip1l in
641 the spinal dorsal or ventral horn of mice from hour 2 to day 14 after subcutaneous
642 injection of CFA. RT-qPCR results showed that circRNA-Filip1l expression in the
643 spinal dorsal horn was not altered in the acute phase (2 h) after CFA injection,
644 however, was increased by 75% day 1, reached a peak (180%) day 3, diminished
645 day 7, and then returned to almost basal level day 14 after CFA injection (Fig. 2*A*).
646 The circRNA-Filip1l level in the ventral horn of spinal cord was increased merely
647 by 60 % day 3 and 53% day 7, but had no change at the other time points after
648 CFA injection (Fig. 2*B*). Furthermore, we found that the expression of

649 circRNA-Filip1l in the contralateral spinal dorsal horn (Fig. 2*C*) and ipsilateral
650 DRG (Fig. 2*D*) was not altered from hour 2 to day 14 after CFA injection. These
651 results suggest that ipsilateral spinal dorsal horn is a major region contributing to
652 the increase of circRNA-Filip1l in chronic inflammation pain. This increase trend of
653 spinal circRNA-Filip1l expression related to chronic pain also was found in
654 ipsilateral spinal dorsal horn of CCI mice (another chronic pain model) day 3, 7
655 and 14 after surgery (Fig. 2*E*), but not observed in the ipsilateral DRG of CCI mice
656 (Fig. 2*F*). These data indicate the possible involvement of spinal circRNA-Filip1l
657 not only in chronic inflammatory pain but also in chronic neuropathic pain. Then,
658 we characterized the differential spatial patterns of expression of spinal
659 circRNA-Filip1l by combining FISH and cell-type-specific immunofluorescence
660 staining *in vivo*. We observed that circRNA-Filip1l was co-localized with NeuN, a
661 neuronal maker, in spinal cord (Fig. 2*G*). To further measure the expression level
662 of circRNA-Filip1l in spinal neurons and non-neurons, we analyzed its content in
663 the cultured spinal neurons and glial cells including astrocytes and microglial cells.
664 As shown in Fig. 2*H*, circRNA-Filip1l in neurons was 7.8 fold as that in microglial
665 cells, and 6.2 fold as that in astrocyte cells, indicating circRNA-Filip1l is mainly
666 expressed in spinal neuron cells. Since the cultured neurons can be depolarized
667 with high concentration KCl to mimic sensitized *in vivo* neurons by nociceptive
668 response (Yang et al., 2015). We treated the cultured spinal neurons with 50 mM
669 KCl for 12 h, and found that circRNA-Filip1l was significantly increased by this

treatment (Fig. 2*I*), supporting a consistent change trend of circRNA-Filip1l expression between the spinal neurons of CFA-treated mice and KCl-treated spinal neurons *in vitro*. In addition, single-cell RT-PCR showed that five of six spinal neurons from CFA mice expressed circRNA-Filip1l (Fig. 2*J*), further confirming that the majority of spinal neurons express circRNA-Filip1l. Collectively, these results suggest that spinal circRNA-Filip1l is increased under chronic pain conditions.

Regulation of nociception by spinal circRNA-Filip1l

To further evaluate the therapeutic potential of spinal circRNA-Filip1l blockade in the relief of nociception response, we used the linear specific antisense of circRNA-Filip1l, including one exogenously synthesized anti-Filip1l by the use of *in vitro* T7 transcription, an antisense RNA of cirRNA-Filip1l that can prevent it from binding to its target gene; and another endogenous PLV-anti-Filip1l with GFP label *in vivo* expressed by lentivirus to block spinal circRNA-Filip1l in CFA mice. The analysis of GFP fluorescence intensity showed that PLV-anti-Filip1l mainly expressed in spinal neurons of naïve mice day 3 after 2 consecutive days' intrathecal injection (Fig. 3*A*). Before the measure of nociceptive behavior, to exclude the possibility that the observed effects were affected by locomotor impairment, we observed the locomotor function in mice by testing their grasping reflex, placing reflex and righting reflex. Results showed that blocking

691 circRNA-Filip1l with anti-Filip1l or PLV-anti-Filip1l did not influence the locomotor
692 function of the mice (Table 1.). Thermal and mechanical nociceptive responses
693 were attenuated hour 24 after intrathecal injections of anti-Filip1l, but not
694 scrambled control in CFA mice, these alleviative effects lasted at least 2 days (Fig.
695 3*B*). The anti-nociceptive effects of PLV-anti-Filip1l were also observed day 2 after
696 intrathecal injection of PLV-anti-Filip1l in CFA mice (Fig. 3*C*), the effects had been
697 maintained during the entire period of observation. To further explore the role of
698 spinal circRNA-Filip1l in nociceptive regulation, then, we examined whether
699 circRNA-Filip1l overexpression mimicks the nociception-like behavior in naïve
700 mice. To this end, two manipulating tools were employed --- exogenous
701 circRNA-Filip1l mimics synthesized through cyclizating the linear circRNA-Filip1l
702 from *in vitro* T7 transcription according to the previous described (Legnini et al.,
703 2017), and endogenous Lenti-Filip1l lentivirus --- to overexpress the
704 circRNA-Filip1l in spinal cord of mice. Validation experiments showed that spinal
705 circRNA-Filip1l expression in naïve mice were up-regulated by 157% day 2 after
706 treatment with circRNA-Filip1l mimics and by 155% day 3 after Lenti-Filip1l
707 treatment, respectively (Fig. 3*D, E*). Similarly, Lenti-Filip1l with GFP label mainly
708 expressed in spinal neurons of naïve mice day 3 after 2 consecutive days'
709 intrathecal injection (Fig. 3*F*). Locomotor impairment was not found after
710 overexpression of spinal circRNA-Filip1l by the use of circRNA-Filip1l mimics or
711 Lenti-Filip1l (Table 1.). However, the intrathecal injections of circRNA-Filip1l

712 mimics or Lenti-Filip1l for 2 or 3 consecutive days, but not scrambled control or
713 empty vector, significantly produced a nociception-like behavior as evidenced by
714 a decrease threshold of mechanical or thermal stimulation (Fig. 3*G, H*). Together,
715 these findings establish that spinal circRNA-Filip1l plays an essential role in
716 physical and pathological nociceptive regulation.
717
718 **MiRNA-1224 is an upstream regulator of circRNA-Filip1l**
719 How is spinal circRNA-Filip1l up-regulated under chronic inflammatory pain
720 conditions? Data from previous study suggest that miRNAs modulate the
721 circRNAs expression via binding to the circRNA in cell nucleus (Hansen et al.,
722 2011). Through search in mirbase database using sequence of circRNA-Filip1l or
723 its precursor (pre-circRNA-Filip1l), we predicted possible miRNAs with the binding
724 sites to circRNA-Filip1l or pre-circRNA-Filip1l. We found that 14nt fragment in
725 miRNA-1224 was complementary to pre-circRNA-Filip1l region spanning its 5'
726 junction flank (Fig. 4*A*). Due to the location of pre-circRNA-Filip1l in spinal nucleus
727 fraction, we supposed that miRNA-1224, as an upstream regulator, may be
728 involved in the modulation of circRNA-Filip1l expression via the mediation of its
729 cleavage. To confirm the existence of miRNA-1224 in spinal nucleus, we detected
730 miRNA-1224 content in both nucleus and cytoplasma of spinal neuron cultured.
731 MiRNA-1224 was mainly located in nucleus, and its level in nucleus was 3.8-fold
732 higher than that in cytoplasma (Fig. 4*B*). FISH further confirmed the preferential

733 localization of miRNA-1224 in nucleus of spinal neurons (Fig. 4*C*). Furthermore,
734 spinal miRNA-1224 expression was time-dependently decreased from hour 2 to
735 day 7 after CFA injection (Fig. 4*D*). Co-staining confirmed that miRNA-1224 was
736 spatially localized in the spinal neurons, and markedly increased under
737 CFA-induced inflammatory pain conditions (Fig. 4*E*).

738 To experimentally validate the *in silicon* prediction of miRNA-1224 regulating
739 circRNA-Filip1le expression, we cloned a bound fragment of pre-circRNA-Filip1l
740 by miRNA-1224 into psiCHECK reporter vector and detected the effect of
741 miRNA-1224 on the activities of the reporter in HEK293T cells. Co-transfection of
742 miRNA-1224 mimics with the reporter psiCK-wt-pre-Filip1l decreased luciferase
743 activities by 39% compared with mutated psiCK-mut-pre-Filip1l vector. Contrarily,
744 miRNA-1224 inhibitor elevated luciferase activities by 52% in psiCK-wt-pre-Filip1l,
745 but not in psiCK-mut-pre-Filip1l (Fig. 4*F*). These data indicate that miRNA-1224 *in*
746 *vitro* negatively regulates the expression of circRNA-Filip1l. To seek to determine
747 whether miRNA-1224 regulates circRNA-Filip1l expression *in vivo* via binding to
748 pre-circRNA-Filip1l, we firstly examined the binding capacity of miRNA-1224 to
749 pre-circRNA-Filip1l. We intrathecally injected bio-labeled miRNA-1224 probes into
750 control and CFA mice, and then tested the content of pre-circRNA-Filip1l
751 pull-down hour 24 after injection. RT-qPCR showed that pre-circRNA-Filip1l was
752 pull down by miRNA-1224 probes, and was increased in spinal cord of CFA mice,
753 compared with saline group (Fig. 4*G*), confirming the binding ability of

754 miRNA-1224 to the pre-circRNA-Filip1l *in vivo*. Next, we further determined if
755 miRNA-1224 can regulate circRNA-Filip1l expression by targeting
756 pre-circRNA-Filip1l. Here, two tools including miRNA-1224 mimics and Lenti-1224
757 were synthesized or constructed as the described methods previously (Pan et al.,
758 2014) to up-regulate the expression of miRNA-1224. Their work efficiencies were
759 validated *in vitro* and *in vivo*. As shown in Figure 5A, HEK-293 cells transfected
760 with miRNA-1224 mimics or Lenti-1224, but not scrambled or empty vector,
761 displayed the increased miRNA-1224 by 118% or 189%, respectively (Fig. 4*H*).
762 The expression of miRNA-1224 was up-regulated by 79% hour 48 after 2
763 consecutive days' miRNA-1224 mimics injection, or by 110% hour 72 after 2
764 consecutive days' Lenti-1224 injection in naïve mice and CFA mice (Fig. 4*I*).
765 Furthermore, we found that overexpressing miRNA-1224 with miRNA-1224
766 mimics or Lenti-1224 in spinal cord of CFA mice blocked the CFA-evoked
767 increase in spinal circRNA-Filip1l expression compared to the scrambled or
768 Lenti-vector group (Fig. 4*J*), however, did not change the increase in spinal
769 pre-circRNA-Filip1l of CFA mice (Fig. 4*K*). In contrast, blocking miRNA-1224 with
770 its inhibitor or PLV-1224 led to the increase of circRNA-Filip1l level (Fig. 4*L*), but
771 unaltered the pre-circRNA-Filip1l level in spinal cord of naïve mice (Fig. 4*M*).
772 Together, these *in vitro* and *in vivo* results indicate miRNA-1224 regulates
773 expression of circRNA-Filip1l, but not pre-circRNA-Filip1l.
774

MiRNA-1224 regulates nociception by mediation of circRNA-Filip1l

Our results indicate that miRNA-1224 modulates spinal circRNA-Filip1l expression under chronic inflammatory pain conditions. Therefore, spinal miRNA-1224 may also participate in the process of nociception regulation. Prior to pain behavior evaluation, we examined the effect of miRNA-1224 regulation tools on locomoter function. The reflex tests showed that miRNA-1224 overexpression with miRNA-1224 mimics or Lenti-1224 did not affect the locomotor function (Table 1.). However, CFA-induced thermal and mechanical nociceptive responses were attenuated hour 48 after the intrathecal injection of miRNA-1224 mimics (Fig. 5*A*) or hour 72 after intrathecal injection of Lenti-1224 (Fig. 5*B*). Anti-nociceptive effect was undetected after the injection of scramble (Fig. 5*A*) or empty vector (Fig. 5*B*). We also observed that pre-treatment with Lenti-1224, not empty vector, (*i.t.* injection of Lenti-1224 or empty vector for 2 consecutive days before CFA injection) significantly prevented CFA-induced nociceptive responses (Fig. 5*C*). Next, we tested whether knockdown of spinal miRNA-1224 in naïve mice can induce the nociception-like behavior. The reflex tests confirmed no impairment of locomotor function after down-regulation of spinal miRNA-1224 expression via intrathecally injecting miRNA-1224 inhibitor or PLV-1224 or their negative controls for 2 consecutive days in naïve mice (Table 1.). While, the same treatment with miRNA-1224 inhibitor (Fig. 5*D*) or PLV-1224 (Fig. 5*E*), but not scramble or empty vector, significantly produced nociceptive responses as evidenced by a decrease

of thermal and mechanical pain threshold (Fig. 5*D, E*). These findings suggest that spinal miRNA-1224 is involved in the process of nociceptive response. Finally, we checked whether miRNA-1224 regulates pain behavior through the mediation of circRNA-Filip1l. Naïve mice were pre-treatment or post-treatment with miRNA-1224 inhibitor or lentivirus to knockdown their spinal miRNA-1224 before or after intrathecal injection of anti-Filip1l, respectively, and then their nociceptive responses were measured. We observed that knockdown of circRNA-Filip1l significantly inhibited or reversed nociceptive responses induced by the block of miRNA-1224 with lentivirus (Fig. 5*F*) or inhibitor (Fig. 5*G*), suggesting that circRNA-Filip1l mediates the regulation of nociception by miRNA-1224. Taken together, these findings indicate that spinal miRNA-1224 regulates nociception via negatively targeting circR-Filip1l.

Ago2-mediated cleavage of pre-circRNA-Filip1l bound by miRNA-1224

To date, the modulatory mechanism of circRNA expression is poorly understood. In recent study, it has been demonstrated that miRNA-671 directs cleavage of a circular antisense transcript of CDR1 in an Ago2-slicer-dependent manner (Hansen et al., 2011). Therefore, we hypothesized that miRNA-1224 mediates the cleavage of pre-circRNA-Filip1l in Ago2-dependent manner to regulate the content of mature circRNA-Filip1l. To test the point, firstly, we co-transfected Ago2 overexpression plasmid (Lenti-Ago2) and miRNA-1224 mimics with wild reporter

psiCK-wt-pre-Filip1l or mutation reporter psiCK-mut-pre-Filip1l in HEK293T cells. The transfection of miRNA-1224 mimics reduced the luciferase activities in psiCK-wt-pre-Filip1l group, compared with psiCK-mut-pre-Filip1l group; the overexpression of Ago2 further decreased the luciferase activities (Fig. 6*A*), suggesting the overexpression of Ago2 inhibits the activity of pre-circRNA-Filip1l expression. We further examined whether Ago2 can combine to pre-cirRNA-Filip1l and miRNA-1224. We used Ago2 antibody to pull down spinal pre-circRNA-Filip1l and miRNA-1224. RNA immunoprecipitation (RPIP) showed that both pre-circRNA-Filip1l and miRNA-1224 were pulled down by Ago2 antibody, and the harvested amounts were decreased in CFA mice compared with saline group (Fig. 6*B*). Next, we investigated whether Ago2 is involved in regulation of circRNA-Filip1l and pre-circRNA-Filip1l expression. Due to the reduced level of spinal Ago2 protein (Fig. 6*C*) day 3 after CFA injection, Lenti-Ago2 or Ago2 protein were intrathecally injected into CFA mice to overexpress Ago2; as well as PLV-Ago2 or Ago2-siRNA into naïve mice to knockdown Ago2 expression, then the effect of Ago2 on expression of circRNA-Filip1l and pre-circRNA-Filip1l were evaluated. The tools of manipulating Ago2 were firstly validated. Ago2 protein was increased by 54% day 2 after intrathecal injection of Lenti-Ago2 in saline group mice; the decreased Ago2 expression was reversed day 3 after the same treatment in CFA mice (Fig. 6*C*), respectively. Ago2 expression was reduced by 41.2% or 39.3% day 2 after

intrathecal injection of Ago2-siRNA or day 3 after PLV-Ago2 injection in naïve mice, respectively (Fig. 6*D*). As expected, compared with the PBS or vector control group, the intrathecal injections of Ago2 protein or Lenti-Ago2 abolished the increase of spinal circRNA-Filip1l (Fig. 6*E*), but did not change the pre-circRNA-Filip1l level (Fig. 6*F*) in CFA mice. Intrathecal injections of Ago2-siRNA or PLV-Ago2 significantly elevated the expression of spinal circRNA-Filip1l (Fig. 6*G*), but not pre-circRNA-Filip1l level in naïve mice (Fig. 6*H*). These results suggest that Ago2 affects the expression of circRNA-Filip1l, but not pre-circRNA-Filip1l. Finally, we wanted to know whether mice receiving the intrathecal injections of manipulation tools of Ago2 display behavioral changes in nociceptive thresholds. We observed that the injections of Ago2 protein (Fig. 6*I*) or Lenti-Ago2 (Fig. 6*J*), but not of PBS (Fig. 6*I*) or Lenti-vector (Fig. 6*J*), significantly blunted the thermal and mechanical nociception, respectively. On the contrary, injections of Ago2-siRNA (Fig. 6*K*) or PLV-Ago2 (Fig. 6*L*), but not of scramble (Fig. 6*K*) or vector (Fig. 6*L*), produced nociceptive responses. To further examine whether Ago2 regulates nociception via the mediation of circRNA-Filip1l or miRNA-1224, we evaluated the effect of blocking circRNA-Filip1l on nociception induced by knockdown of Ago2. As expected, blockage of circRNA-Filip1l by intrathecal pre-injection of anti-Filip1l prevented nociceptive responses induced by Ago2 down-regulation in naïve mice (Fig. 6*M*). However, overexpression of spinal miRNA-1224 with Lenti-1224 did not prevent nociception induced by

Ago2-siRNA in naïve mice (Fig. 6*N*), indicating Ago2 regulates nociceptive responses via circRNA-Filip1l, but not miRNA-1224. Collectively, these findings suggest that Ago2 is involved in regulation of physical and pathological nociception via miRNA-1224-dependent cleavage in circRNA-Filip1l.

CircRNA-Filip1l regulates nociception via targeting Ubr5

Many recent studies (Li et al., 2015; Long et al., 2017) have shown that nucleus circRNAs contribute to gene transcription via recruiting the RNA polymerase II. Therefore, we wanted to know what are the downstream of circRNA-Filip1l underlying regulation of nociception. Firstly, we performed an *in silicon* target prediction using linear sequence of circRNA-Filip1l in BLAST program of NCBI. A total of 42 genes were predicted as the potential targets of circRNA-Filip1l. Some (e.g., Rn28s1, LOC105242388) are the ribosomal RNA or noncoding RNA, others are the unreported pain-related genes such as Atxn2，Pwwp2a，Plxdc2 and Ubr5. Among them, ubiquitin protein ligase E3 component n-recognin 5 (Ubr5) can regulate the neuronal plasticity through activating the NMDA receptor in CNS, and is implicated in the pathologic process of central neural system diseases such as depression and epilepsy through ubiquitination of modification (Kato et al., 2012; Christensen et al., 2013). In Ubr5 gene, the specific region near transcription start site (TSS) of Ubr5 (+221 - +242, TSS as +1) was found to be bound by circRNA-Filip1l (+25 - +4, 5' junction as +1) (Fig. 7*A*). Therefore, we chose to

880 evaluate the potential role of Ubr5 as a target of circRNA-Filip1l. We hypothesized
881 that circRNA-Filip1l facilitates the transcription of Ubr5 through its binding to Ubr5
882 TSS and recruits RNA polymerase. Secondly, to experimentally validate the *in*
883 *silicon* predictions, according to our previous method (Pan et al., 2016), we cloned
884 a 440 bp Ubr5 fragment containing the bound region by circRNA-Filip1l into pGL6
885 reporter vector, and tested the effects of circRNA-Filip1l on the activities of the
886 Ubr5 transcription in HEK293T cells. Expectedly, only pGL6-Ubr5 produced the
887 relative strong luciferase activities compared with the empty vector (Figure 7*B*),
888 indicating the cloned region contains the regulatory element, and can drive Ubr5
889 expression. The co-transfection of pGL6-Ubr5 with circRNA-Filip1l
890 overexpression plasmid enhanced the luciferase activities by 55.7% compared
891 with co-transfection of pGL6-Ubr5 with empty vector (Fig. 7*B*). Thirdly, we
892 assessed whether Ubr5 co-express with other regulators, single-cell RT-PCR
893 showed that five of six spinal neurons expressed Ubr5, that four of these five cells
894 co-expressed with circRNA-Filip1l, five of them with miRNA-1224, and four of
895 them with Ago2 (Fig. 7*C*), suggesting they are able to co-express in the spinal
896 neurons. Thus, we further examined whether circRNA-Filip1l is involved in the
897 regulation of Ubr5 expression *in vivo*. Spinal Ubr5 was significantly increased by
898 67 % day 3 after CFA injection (Fig. 7*D, E*), suggesting its possible regulatory role
899 in the chronic inflammation pain. Furthermore, the increase of Ubr5 expression
900 was efficiently reversed to the almost basal level day 2 after intrathecal injection of

Ubr5-siRNA (Fig. 7*D*) day 3 after intrathecal injection of PLV-Ubr5 (Lentivirus Ubr5-shRNA) in CFA mice (Fig. 7*E*). It is apparent from our data that Ubr5-siRNA- or PLV-Ubr5-, but not scramble- or empty vector-injected mice exhibited the anti-nociceptive effects in CFA-induced chronic inflammatory pain model (Fig. 7*F, G*). These findings indicate the involvement of Ubr5 in the process of chronic pain.

Next, we determined whether there is a regulatory role of circRNA-Filip1l in Ubr5 expression *in vivo*. The increase of Ubr5 was abolished by intrathecal injections of anti-Filip1l, but not the scrambled control in CFA mice (Fig. 7*H*). While, overexpressing circRNA-Filip1l with circRNA-Filip1l mimics (Fig. 7*I*) or Lenti-Filip1l (Fig. 7*J*) reduced the level of Ubr5 protein, compared with scrambled or empty vector in naïve mice, suggesting that Ubr5 is a positive regulatory target of circRNA-Filip1l. Finally, to explore the role of Ubr5 in mediating nociceptive regulation by circRNA-Filip1l, we pre- or post- treated animals with Ubr5-siRNA before or after overexpressing spinal circRNA-Filip1l, and then measured the nociceptive responses. Behavioral results showed that the knockdown of Ubr5 with intrathecal pre-treatment with PLV-Ubr5 significantly prevented thermal and mechanical nociceptive responses induced by overexpression of circRNA-Filip1l through *i.t.* injection of its mimics (Fig. 7*K*). Moreover, down-regulation of Ubr5 with PLV-Ubr5 post-treatment significantly alleviated thermal and mechanical nociceptive responses induced by Lenti-Filip1l (Fig. 7*L*). These findings indicate a direct mediatory role of Ubr5 in regulation of nociception by circRNA-Filip1l.

Together, these results suggest that spinal circRNA-Filip1l regulates nociception via positively targeting Ubr5. In conclusion, these data indicate that miRNA-1224 and Ago2 are involved in the regulation of circRNA-Filip1l-mediated Ubr5 expression (Fig. 8).

Discussion

Chronic pain is one of the most intractable human complaints and is caused by inflammation, lesion or dysfunction of the nervous system (Clark, 2016; Ji et al., 2018; Jing et al., 2018). The expression of aberrant pain-related gene in spinal neuronal or glial cells is the most prominent contributor in various nociceptive pathways underlying chronic pain (Ji et al., 2016; Jiang et al., 2017; Tsuda, 2018). Therefore, the unraveling of the genetic basis and its regulatory mechanisms will improve our insight into chronic pain, and provides potential targets for developing novel therapeutic strategies. Various studies have refined our understanding of miRNAs or long strand ncRNA in the pathway of different pain models, and shown that noncoding RNAs have regulatory functions in the process of nociceptive signal. The current study identified an essential role of circRNA-Filip1l as a mediator of chronic inflammation pain by directly targeting Ubr5 at the spinal level. We further found that miRNA-1224 was an upstream regulator of circRNA-Filip1l in the Ago2-depedent manner. Our results are for the first time to functionally demonstrate that circRNA is an important player to the induction and maintenance of chronic pain.

CircRNA, a noncoding RNA as the novel regulatory mechanism of gene expression, attracts widespread attention on their vital roles in biological processes and human diseases. A growing body of evidence suggests that circRNAs are enriched in nervous system, such as different brain regions, primary

964 neurons and isolated synapses (Shao and Chen, 2016), and a number of
965 circRNAs are highly conservation among species, and their expressions are
966 changed during neuronal differentiation (Rybak-Wolf et al., 2015). However, it is
967 only beginning to understand how circRNAs are involved in physiological and
968 pathological processes of nervous system. Several studies have gained an insight
969 into the function of circRNAs in neurological disorders or diseases like
970 Parkinson's disease (Kumar et al., 2018), Alzheimer's disease (Lu and Xu, 2016;
971 Zhao et al., 2016), amyotrophic lateral sclerosis and spinal muscul aratrophy
972 (Scotti and Swanson, 2016). In 2017, circRNA is firstly reported to be associated
973 with brain function --- circRNA-Cdr1as-knockout mice display the impaired
974 sensorimotor gating due to the dysfunction of excitatory synaptic transmission in
975 brain (Piwecka et al., 2017), circRNA serves as a critical player in CNS diseases.
976 Recent work has focused on the relationship between circRNA and pain. Zhou *et*
977 *al* (Zhou et al., 2017) and Cao *et al* (Cao et al., 2017) found that spared nerve
978 injury (SNI)- or chronic constriction injury-induced neuropathic pain causes the
979 expression alteration of 188 or 469 spinal circRNAs, respectively. Despite spinal
980 circRNA profiles are changed in chronic neuropathic pain, it remains unknown
981 whether circRNAs regulate the nociception behavior. The results of this study
982 showed that CFA-induced chronic inflammation pain increased the content of
983 circRNA-Filip1l in spinal cord of mice; knockdown of circRNA-Filip1l alleviated the

984 nociceptive behavior, supporting the idea that circRNA-Filip1l regulates the
985 nociceptive response.

986 MiRNAs are approximately 21 nucleotides in length and well-studied
987 noncoding RNA species in terms of their biogenesis and functions. Increasing
988 evidence over the past few years from different pain models have linked miRNA to
989 nociceptive pathways including membrane receptors (Park et al., 2014; Jiang et
990 al., 2016), ion channels (Pan et al., 2016; Peng et al., 2017), transcription factors
991 (Willemen et al., 2012), translation factors (Sun et al., 2012), and other cellular
992 signals (Zhou et al., 2016), from primary afferent nociceptors, DRG, spinal cord,
993 and brain areas. Previous reports on nucleus miRNAs uncover their importance
994 functions in the RNA splice or transcription (Liao et al., 2010). For example,
995 nucleus miR-671 can mediate the cleavage of circRNA-Cdr1as in mouse brain
996 (Hansen et al., 2011). Although growing number of molecular and functional data
997 support the involvement of cytoplasma miRNA in the process of chronic pain, little
998 is known about whether nucleus miRNA is related to chronic pain. In our work, the
999 abundant expression of miRNA-1224 was identified in the mouse spinal nucleus.
1000 Indeed, miRNA-1224 has been discovered to differentially express in the liver of
1001 fatty liver disease (Dolganiuc et al., 2009), and in different tissues of bladder
1002 cancer (Dudziec et al., 2011), inflammation and acute injured kidney (Niu et al.,
1003 2011; Bellinger et al., 2014; Roy et al., 2017). MiRNA-1224 can be also detected
1004 in hippocampus and the marginal division of the neostriatum in rats (Shu et al.,

2013). But, Up to now, far too little attention has been paid to the function of miRNA-1224 in diseases. We provide the first evidence that spinal nucleus miRNA-1224 is implicated in the modulation of chronic inflammatory pain. Furthermore, we reveal a novel mechanism of miRNA-122 in the pain process through splicing circRNA-Filip1l in Ago2-depedent manner.

In fact, it is still challenged to understand how circRNA expression itself is regulated in pathological processes. Several reports show that antisense oligonucleotide or miRNA are associated with the splice of circRNA, and change their expression level (Havens et al., 2013; Jeck and Sharpless, 2014). As miRNA-671 almost fully binds to circRNA-Cdr1as to form the miRNA-671-circRNA-Cdr1as complex in cell nucleus, Ago2 slices circRNA-Cdr1as after recognizing the complex (Piwecka et al., 2017). In the present study, we found that Ago2 recognized and sliced the complex formed by miRNA-1224 and pre-circRNA-Filip1l, resulting in the reduction of mature circRNA-Filip1l in the spinal nucleus. Our data suggest that miRNA-mediated Ago2 cleavage for pre-circRNA may play a crucial role in the modulation of circRNA biogenesis, at the least, in spinal nucleus. Therefore, combined with previous reports, circRNA may be regulated through two ways: Ago2 cleaved circRNA or their precursors after miRNAs binding. Our findings will allow for a new optional strategy in prevention and treatment of pain or other CNS diseases via affecting circRNA biogenesis by miRNA.

Ago2, termed as EIF2C2, is a member of Ago family (1, 2, 3 and 4) characterized with a high conservation among species and broadly expression in different tissues (Ye et al., 2015). Interestingly, Ago2 is the only one with catalytic activity among family members, and efficiently silences the expression of small RNAs. Distinguishing from the other members, mice with Ago2 knockout are lethal (Shekar et al., 2011). Extensive studies have shown that Ago2 participates in miRNA generation (Schaefer et al., 2010), miRNA-mediated mRNA degradation (Meister et al., 2004; Cifuentes et al., 2010), translation repression (Friend et al., 2012), and hetero-chromatinization (Moshkovich et al., 2011) in Dicer (an endoribonuclease)-independent means. Knockdown of Ago2 leads to the decrease of global miRNA (Morita et al., 2007). For example, Ago2, not 1, 3 and 4, is down-regulated in brain lysates from encephalomyelitis mice, the expression level of several miRNAs including let-7a-5p, let-7e-5p, let-7f-5p, 106b-5p, 144-3p, and 188a-5p display a significant reduction (Lewkowicz et al., 2015), suggesting Ago2 is involved in the etiology of CNS diseases (Savas et al., 2008). Deficiency of Ago2 in D2R neurons relieves self-administration of cocaine due to the declined content of miRNAs in the mouse striatum (Schaefer et al., 2010), revealing a vital role of Ago2 in the treatment of CNS diseases (Carrick et al., 2016). Here, we found nociceptive behavior caused the decrease of spinal Ago2 level, and overexpressing Ago2 significantly attenuated the pain hypersensitivity, it can

1046 therefore be concluded that Ago2 is a an important player in nociceptive
1047 response.

1048 Despite a large number of circRNAs have been found, how circRNA regulates
1049 gene expression is a major problem for a long time. The relatively well-studied
1050 mechanism is that circRNA adsorbs miRNAs (a process known as miRNA
1051 sponge), and thereby decreases the binding of miRNAs to their target mRNAs
1052 (Hansen et al., 2013b). As circRNA-HIPK3 adsorbs 9 different miRNAs, the
1053 knockdown of circRNA-HIPK3 inhibits cell growth via enhancing the level of
1054 miRNAs binding to the target mRNAs (Zheng et al., 2016). MiRNA-7 is involved in
1055 the formation of dendritic spine density (Choi et al., 2015; Zhang et al., 2015),
1056 Cdr1as is known as the sponge for miRNA-7 and regulates the stability or
1057 transport of miRNA-7 in neuronal cells, hence, the function-loss-circRNA-Cdr1as
1058 impairs the sensorimotor gating and synaptic transmission of mouse brain tissues
1059 including cerebellum, cortex, hippocampus, and olfactory bulb by enhancing the
1060 number of freely available miRNA-7 (Piwecka et al., 2017). Although, relatively to
1061 act as sponge of miRNAs, only few circRNAs are studied in the function of gene
1062 transcription, it is now well established from various studies that circRNAs can
1063 bind to not only proteins such as AGO and RNA polymerase II (PolI), but also to
1064 linear RNAs and DNAs in cellular nucleus. CircRNA from *Fmn* gene lavishly
1065 presents in nucleus, and promotes the transcription of *Fmn* gene by enhancing
1066 the binding capacity of PolI to *Fmn* promoter (Chao et al., 1998; Zhang et al.,

2013). Similarly, the complex formed by circRNA-EI and U1 snRNP can also recruit PolI to the promoter of circRNA-EI parental gene in nucleus, initiating the transcription process (Li et al., 2015). Interestingly, circRNA-Mble regulates the biogenesis of parent linear Mble RNA (Ashwal-Fluss et al., 2014). Consistently, our findings showed that circRNA-Filip1l enhanced the transcription level of Ubr5 via binding to the near region in TSS. But, further research should be undertaken to investigate whether the binding sites recruit the RNA polymerase. Our observations may provide an approach to obtain the possible downstream targets of nucleus circRNAs. The findings of the current study support the previous reports: such lncRNAs as RoX2, TERC, and HOTAIR, are enriched in the mammalian nucleus, and bind to gene bodies and GA-rich DNA regions to control gene transcription via recruiting RNA polymerase (Chu et al., 2011; Bonasio and Shiekhattar, 2014). Consequently, we speculate that circRNA or lncRNA may share the regulatory mechanism of gene expression through transcriptional interference (Bonasio and Shiekhattar, 2014; Fatica and Bozzoni, 2014).

Ubr5 is a HECT (homologous to E6-associated protein at the carboxy-terminus) E3 Ub ligase recognizing n-degrons, and has a catalytic ability of directly recognizing and ligating ubiquitin to degrading proteins. It is very well deliberated that Ubr5 participates in CNS-related diseases, such as neuroinflammation, cognitive disorders and depression (Gudjonsson et al., 2012; Rutz et al., 2015). Depression increases Ubr5 expression in the lateral habenula

tissues of rats, the administration of Escitalopram, a selective serotonin reuptake inhibitor, for 4 weeks alleviates the depression behavior by decreasing the level of Ubr5 expression (Christensen et al., 2013). Ubr5 mutation clinically impairs the cognitive capability in Alzheimer disease (Hu et al., 2011), suggesting Ubr5 has an essential role in CNS diseases. In our work, Ubr5 was significantly increased in spinal cord of chronic inflammatory pain model, the knockdown of Ubr5 attenuated the pain behavior, and therefore, Ubr5 could serve as an important regulator in the process chronic pain.

In summary, we demonstrate that spinal miRNA-1224-mediated splice of circRNA-Filip1l in Ago2-depedent manner regulate chronic inflammatory pain via targeting Ubr5. These findings shed light on new circRNA mechanism underlying nociceptive information processing; may provide a rational for the future development of potential targeted interventions via circRNA modulating pain-related gene expression.

Reference

Ashwal-Fluss R, Meyer M, Pamudurti NR, Ivanov A, Bartok O, Hanan M, Evantal N, Memczak S, Rajewsky N, Kadener S (2014) circRNA biogenesis competes with pre-mRNA splicing. Molecular cell 56:55-66.

Bellinger MA, Bean JS, Rader MA, Heinz-Taheny KM, Nunes JS, Haas JV, Michael LF, Rekhter MD (2014) Concordant changes of plasma and kidney microRNA in the early stages of acute kidney injury: time course in a mouse model of bilateral renal ischemia-reperfusion. PloS one 9:e93297.

Bonasio R, Shiekhattar R (2014) Regulation of transcription by long noncoding RNAs. Annual review of genetics 48:433-455.

Cao S, Deng W, Li Y, Qin B, Zhang L, Yu S, Xie P, Xiao Z, Yu T (2017) Chronic constriction injury of sciatic nerve changes circular RNA expression in rat spinal dorsal horn. Journal of pain research 10:1687-1696.

Carrick WT, Burks B, Cairns MJ, Kocerha J (2016) Noncoding RNA Regulation of Dopamine Signaling in Diseases of the Central Nervous System. Frontiers in molecular biosciences 3:69.

Chao CW, Chan DC, Kuo A, Leder P (1998) The mouse formin (Fmn) gene: abundant circular RNA transcripts and gene-targeted deletion analysis. Molecular medicine 4:614-628.

Chen W, Schuman E (2016) Circular RNAs in Brain and Other Tissues: A Functional Enigma. Trends in neurosciences 39:597-604.

Choi SY, Pang K, Kim JY, Ryu JR, Kang H, Liu Z, Kim WK, Sun W, Kim H, Han K (2015) Post-transcriptional regulation of SHANK3 expression by microRNAs related to multiple neuropsychiatric disorders. Molecular brain 8:74.

Christensen T, Jensen L, Bouzinova EV, Wiborg O (2013) Molecular profiling of the lateral habenula in a rat model of depression. PloS one 8:e80666.

Chu C, Qu K, Zhong FL, Artandi SE, Chang HY (2011) Genomic maps of long noncoding RNA occupancy reveal principles of RNA-chromatin interactions. Molecular cell 44:667-678.

Cifuentes D, Xue H, Taylor DW, Patnode H, Mishima Y, Cheloufi S, Ma E, Mane S, Hannon GJ, Lawson ND, Wolfe SA, Giraldez AJ (2010) A novel miRNA processing pathway independent of Dicer requires Argonaute2 catalytic activity. Science 328:1694-1698.

Clark JD (2016) Preclinical Pain Research: Can We Do Better? Anesthesiology 125:846-849.

Descalzi G, Ikegami D, Ushijima T, Nestler EJ, Zachariou V, Narita M (2015) Epigenetic mechanisms of chronic pain. Trends in neurosciences 38:237-246.

Dolganiuc A, Petrasek J, Kodys K, Catalano D, Mandrekar P, Velayudham A, Szabo G (2009) MicroRNA expression profile in Lieber-DeCarli diet-induced alcoholic and methionine choline deficient diet-induced nonalcoholic steatohepatitis models in mice. Alcoholism, clinical and experimental research 33:1704-1710.

Dudziec E, Miah S, Choudhry HM, Owen HC, Blizard S, Glover M, Hamdy FC, Catto JW (2011) Hypermethylation of CpG islands and shores around specific microRNAs and mirtrons is associated with the phenotype and presence of bladder cancer. Clinical cancer research : an official journal of the American Association for Cancer Research 17:1287-1296.

Fatica A, Bozzoni I (2014) Long non-coding RNAs: new players in cell differentiation and development. Nature reviews Genetics 15:7-21.

1149 Friend K, Campbell ZT, Cooke A, Kroll-Conner P, Wickens MP, Kimble J (2012) A conserved PUF-Ago-eEF1A
1150 complex attenuates translation elongation. Nature structural & molecular biology 19:176-183.
1151 Gandla J, Lomada SK, Lu J, Kuner R, Bali KK (2017) miR-34c-5p functions as pronociceptive microRNA in
1152 cancer pain by targeting Cav2.3 containing calcium channels. Pain.
1153 Glazar P, Papavasileiou P, Rajewsky N (2014) circBase: a database for circular RNAs. Rna 20:1666-1670.
1154 Gudjonsson T, Altmeyer M, Savic V, Toledo L, Dinant C, Grofte M, Bartkova J, Poulsen M, Oka Y,
1155 Bekker-Jensen S, Mailand N, Neumann B, Heriche JK, Shearer R, Saunders D, Bartek J, Lukas J,
1156 Lukas C (2012) TRIP12 and UBR5 suppress spreading of chromatin ubiquitylation at damaged
1157 chromosomes. Cell 150:697-709.
1158 Hansen TB, Kjems J, Damgaard CK (2013a) Circular RNA and miR-7 in cancer. Cancer research
1159 73:5609-5612.
1160 Hansen TB, Wiklund ED, Bramsen JB, Villadsen SB, Statham AL, Clark SJ, Kjems J (2011) miRNA-dependent
1161 gene silencing involving Ago2-mediated cleavage of a circular antisense RNA. The EMBO journal
1162 30:4414-4422.
1163 Hansen TB, Jensen TI, Clausen BH, Bramsen JB, Finsen B, Damgaard CK, Kjems J (2013b) Natural RNA
1164 circles function as efficient microRNA sponges. Nature 495:384-388.
1165 Havens MA, Duelli DM, Hastings ML (2013) Targeting RNA splicing for disease therapy. Wiley
1166 interdisciplinary reviews RNA 4:247-266.
1167 Holdt LM, Stahringer A, Sass K, Pichler G, Kulak NA, Wilfert W, Kohlmaier A, Herbst A, Northoff BH,
1168 Nicolaou A, Gabel G, Beutner F, Scholz M, Thiery J, Musunuru K, Krohn K, Mann M, Teupser D
1169 (2016) Circular non-coding RNA ANRIL modulates ribosomal RNA maturation and atherosclerosis
1170 in humans. Nature communications 7:12429.
1171 Hu X, Pickering EH, Hall SK, Naik S, Liu YC, Soares H, Katz E, Paciga SA, Liu W, Aisen PS, Bales KR, Samad TA,
1172 John SL (2011) Genome-wide association study identifies multiple novel loci associated with
1173 disease progression in subjects with mild cognitive impairment. Translational psychiatry 1:e54.
1174 Hugel S, Schlichter R (2000) Presynaptic P2X receptors facilitate inhibitory GABAergic transmission
1175 between cultured rat spinal cord dorsal horn neurons. The Journal of neuroscience : the official
1176 journal of the Society for Neuroscience 20:2121-2130.
1177 Hunsberger JG, Fessler EB, Wang Z, Elkahloun AG, Chuang DM (2012) Post-insult valproic acid-regulated
1178 microRNAs: potential targets for cerebral ischemia. American journal of translational research
1179 4:316-332.
1180 Imai S et al. (2013) Epigenetic transcriptional activation of monocyte chemotactic protein 3 contributes to
1181 long-lasting neuropathic pain. Brain : a journal of neurology 136:828-843.
1182 Jeck WR, Sharpless NE (2014) Detecting and characterizing circular RNAs. Nature biotechnology
1183 32:453-461.
1184 Ji RR, Chamessian A, Zhang YQ (2016) Pain regulation by non-neuronal cells and inflammation. Science
1185 354:572-577.
1186 Ji RR, Nackley A, Huh Y, Terrando N, Maixner W (2018) Neuroinflammation and Central Sensitization in
1187 Chronic and Widespread Pain. Anesthesiology.
1188 Jiang BC, He LN, Wu XB, Shi H, Zhang WW, Zhang ZJ, Cao DL, Li CH, Gu J, Gao YJ (2017) Promoted
1189 Interaction of C/EBPalpha with Demethylated Cxcr3 Gene Promoter Contributes to Neuropathic

Pain in Mice. The Journal of neuroscience : the official journal of the Society for Neuroscience 37:685-700.

Jiang BC, Cao DL, Zhang X, Zhang ZJ, He LN, Li CH, Zhang WW, Wu XB, Berta T, Ji RR, Gao YJ (2016) CXCL13 drives spinal astrocyte activation and neuropathic pain via CXCR5. The Journal of clinical investigation 126:745-761.

Jing PB, Cao DL, Li SS, Zhu M, Bai XQ, Wu XB, Gao YJ (2018) Chemokine Receptor CXCR3 in the Spinal Cord Contributes to Chronic Itch in Mice. Neuroscience bulletin 34:54-63.

Kato T, Tamiya G, Koyama S, Nakamura T, Makino S, Arawaka S, Kawanami T, Tooyama I (2012) UBR5 Gene Mutation Is Associated with Familial Adult Myoclonic Epilepsy in a Japanese Family. ISRN neurology 2012:508308.

Kumar L, Shamsuzzama, Jadiya P, Haque R, Shukla S, Nazir A (2018) Functional Characterization of Novel Circular RNA Molecule, circzip-2 and Its Synthesizing Gene zip-2 in C. elegans Model of Parkinson's Disease. Molecular neurobiology.

Legnini I, Di Timoteo G, Rossi F, Morlando M, Briganti F, Sthandier O, Fatica A, Santini T, Andronache A, Wade M, Laneve P, Rajewsky N, Bozzoni I (2017) Circ-ZNF609 Is a Circular RNA that Can Be Translated and Functions in Myogenesis. Molecular cell 66:22-37 e29.

Lewkowicz P, Cwiklinska H, Mycko MP, Cichalewska M, Domowicz M, Lewkowicz N, Jurewicz A, Selmaj KW (2015) Dysregulated RNA-Induced Silencing Complex (RISC) Assembly within CNS Corresponds with Abnormal miRNA Expression during Autoimmune Demyelination. The Journal of neuroscience : the official journal of the Society for Neuroscience 35:7521-7537.

Li Z, Huang C, Bao C, Chen L, Lin M, Wang X, Zhong G, Yu B, Hu W, Dai L, Zhu P, Chang Z, Wu Q, Zhao Y, Jia Y, Xu P, Liu H, Shan G (2015) Exon-intron circular RNAs regulate transcription in the nucleus. Nature structural & molecular biology 22:256-264.

Liao JY, Ma LM, Guo YH, Zhang YC, Zhou H, Shao P, Chen YQ, Qu LH (2010) Deep sequencing of human nuclear and cytoplasmic small RNAs reveals an unexpectedly complex subcellular distribution of miRNAs and tRNA 3' trailers. PloS one 5:e10563.

Long Y, Wang X, Youmans DT, Cech TR (2017) How do lncRNAs regulate transcription? Science advances 3:eaao2110.

Lu D, Xu AD (2016) Mini Review: Circular RNAs as Potential Clinical Biomarkers for Disorders in the Central Nervous System. Frontiers in genetics 7:53.

Meister G, Landthaler M, Patkaniowska A, Dorsett Y, Teng G, Tuschl T (2004) Human Argonaute2 mediates RNA cleavage targeted by miRNAs and siRNAs. Molecular cell 15:185-197.

Memczak S, Jens M, Elefsinioti A, Torti F, Krueger J, Rybak A, Maier L, Mackowiak SD, Gregersen LH, Munschauer M, Loewer A, Ziebold U, Landthaler M, Kocks C, le Noble F, Rajewsky N (2013) Circular RNAs are a large class of animal RNAs with regulatory potency. Nature 495:333-338.

Monif M, Reid CA, Powell KL, Drummond KJ, O'Brien TJ, Williams DA (2016) Interleukin-1beta has trophic effects in microglia and its release is mediated by P2X7R pore. Journal of neuroinflammation 13:173.

Morita S, Horii T, Kimura M, Goto Y, Ochiya T, Hatada I (2007) One Argonaute family member, Eif2c2 (Ago2), is essential for development and appears not to be involved in DNA methylation. Genomics 89:687-696.

1231 Moshkovich N, Nisha P, Boyle PJ, Thompson BA, Dale RK, Lei EP (2011) RNAi-independent role for
1232 Argonaute2 in CTCF/CP190 chromatin insulator function. Genes & development 25:1686-1701.
1233 Niu Y, Mo D, Qin L, Wang C, Li A, Zhao X, Wang X, Xiao S, Wang Q, Xie Y, He Z, Cong P, Chen Y (2011)
1234 Lipopolysaccharide-induced miR-1224 negatively regulates tumour necrosis factor-alpha gene
1235 expression by modulating Sp1. Immunology 133:8-20.
1236 Pan Z, Xue ZY, Li GF, Sun ML, Zhang M, Hao LY, Tang QQ, Zhu LJ, Cao JL (2017) DNA Hydroxymethylation by
1237 Ten-eleven Translocation Methylcytosine Dioxygenase 1 and 3 Regulates Nociceptive Sensitization
1238 in a Chronic Inflammatory Pain Model. Anesthesiology 127:147-163.
1239 Pan Z, Zhang M, Ma T, Xue ZY, Li GF, Hao LY, Zhu LJ, Li YQ, Ding HL, Cao JL (2016) Hydroxymethylation of
1240 microRNA-365-3p Regulates Nociceptive Behaviors via Kcnh2. The Journal of neuroscience : the
1241 official journal of the Society for Neuroscience 36:2769-2781.
1242 Pan Z, Zhu LJ, Li YQ, Hao LY, Yin C, Yang JX, Guo Y, Zhang S, Hua L, Xue ZY, Zhang H, Cao JL (2014) Epigenetic
1243 modification of spinal miR-219 expression regulates chronic inflammation pain by targeting
1244 CaMKIIgamma. The Journal of neuroscience : the official journal of the Society for Neuroscience
1245 34:9476-9483.
1246 Park CK, Xu ZZ, Berta T, Han Q, Chen G, Liu XJ, Ji RR (2014) Extracellular microRNAs activate nociceptor
1247 neurons to elicit pain via TLR7 and TRPA1. Neuron 82:47-54.
1248 Peng C, Li L, Zhang MD, Bengtsson Gonzales C, Parisien M, Belfer I, Usoskin D, Abdo H, Furlan A, Haring M,
1249 Lallemend F, Harkany T, Diatchenko L, Hokfelt T, Hjerling-Leffler J, Ernfors P (2017) miR-183 cluster
1250 scales mechanical pain sensitivity by regulating basal and neuropathic pain genes. Science
1251 356:1168-1171.
1252 Piwecka M, Glazar P, Hernandez-Miranda LR, Memczak S, Wolf SA, Rybak-Wolf A, Filipchyk A, Klironomos F,
1253 Cerda Jara CA, Fenske P, Trimbuch T, Zywitza V, Plass M, Schreyer L, Ayoub S, Kocks C, Kuhn R,
1254 Rosenmund C, Birchmeier C, Rajewsky N (2017) Loss of a mammalian circular RNA locus causes
1255 miRNA deregulation and affects brain function. Science 357.
1256 Rasko JE, Wong JJ (2017) Nuclear microRNAs in normal hemopoiesis and cancer. Journal of hematology &
1257 oncology 10:8.
1258 Roberts TC (2014) The MicroRNA Biology of the Mammalian Nucleus. Molecular therapy Nucleic acids
1259 3:e188.
1260 Roy S, Bantel H, Wandrer F, Theres Schneider A, Gautheron J, Vucur M, Tacke F, Trautwein C, Luedde T,
1261 Roderburg C (2017) miR-1224 inhibits cell proliferation in acute liver failure by targeting the
1262 antiapoptotic gene Nfib. Journal of hepatology.
1263 Rutz S et al. (2015) Deubiquitinase DUBA is a post-translational brake on interleukin-17 production in T
1264 cells. Nature 518:417-421.
1265 Rybak-Wolf A, Stottmeister C, Glazar P, Jens M, Pino N, Giusti S, Hanan M, Behm M, Bartok O, Ashwal-Fluss
1266 R, Herzog M, Schreyer L, Papavasileiou P, Ivanov A, Ohman M, Refojo D, Kadener S, Rajewsky N
1267 (2015) Circular RNAs in the Mammalian Brain Are Highly Abundant, Conserved, and Dynamically
1268 Expressed. Molecular cell 58:870-885.
1269 Savas JN, Makusky A, Ottosen S, Baillat D, Then F, Krainc D, Shiekhattar R, Markey SP, Tanese N (2008)
1270 Huntington's disease protein contributes to RNA-mediated gene silencing through association

with Argonaute and P bodies. Proceedings of the National Academy of Sciences of the United States of America 105:10820-10825.

Schaefer A, Im HI, Veno MT, Fowler CD, Min A, Intrator A, Kjems J, Kenny PJ, O'Carroll D, Greengard P (2010) Argonaute 2 in dopamine 2 receptor-expressing neurons regulates cocaine addiction. The Journal of experimental medicine 207:1843-1851.

Scotti MM, Swanson MS (2016) RNA mis-splicing in disease. Nature reviews Genetics 17:19-32.

Shao Y, Chen Y (2016) Roles of Circular RNAs in Neurologic Disease. Frontiers in molecular neuroscience 9:25.

Shekar PC, Naim A, Sarathi DP, Kumar S (2011) Argonaute-2-null embryonic stem cells are retarded in self-renewal and differentiation. Journal of biosciences 36:649-657.

Shu SY, Qing D, Wang B, Zeng QY, Chen YC, Jin Y, Zeng CC, Bao R (2013) Comparison of microRNA expression in hippocampus and the marginal division (MrD) of the neostriatum in rats. Journal of biomedical science 20:9.

Sibley CR, Seow Y, Curtis H, Weinberg MS, Wood MJ (2012) Silencing of Parkinson's disease-associated genes with artificial mirtron mimics of miR-1224. Nucleic acids research 40:9863-9875.

Su X, Wang H, Ge W, Yang M, Hou J, Chen T, Li N, Cao X (2015) An In Vivo Method to Identify microRNA Targets Not Predicted by Computation Algorithms: p21 Targeting by miR-92a in Cancer. Cancer research 75:2875-2885.

Sun Y, Li XQ, Sahbaie P, Shi XY, Li WW, Liang DY, Clark JD (2012) miR-203 regulates nociceptive sensitization after incision by controlling phospholipase A2 activating protein expression. Anesthesiology 117:626-638.

Tao YX, Rumbaugh G, Wang GD, Petralia RS, Zhao C, Kauer FW, Tao F, Zhuo M, Wenthold RJ, Raja SN, Huganir RL, Bredt DS, Johns RA (2003) Impaired NMDA receptor-mediated postsynaptic function and blunted NMDA receptor-dependent persistent pain in mice lacking postsynaptic density-93 protein. The Journal of neuroscience : the official journal of the Society for Neuroscience 23:6703-6712.

Tsuda M (2018) Modulation of Pain and Itch by Spinal Glia. Neuroscience bulletin 34:178-185.

Willemen HL, Huo XJ, Mao-Ying QL, Zijlstra J, Heijnen CJ, Kavelaars A (2012) MicroRNA-124 as a novel treatment for persistent hyperalgesia. Journal of neuroinflammation 9:143.

Yang JX, Hua L, Li YQ, Jiang YY, Han D, Liu H, Tang QQ, Yang XN, Yin C, Hao LY, Yu L, Wu P, Shao CJ, Ding HL, Zhang YM, Cao JL (2015) Caveolin-1 in the anterior cingulate cortex modulates chronic neuropathic pain via regulation of NMDA receptor 2B subunit. The Journal of neuroscience : the official journal of the Society for Neuroscience 35:36-52.

Ye Z, Jin H, Qian Q (2015) Argonaute 2: A Novel Rising Star in Cancer Research. Journal of Cancer 6:877-882.

You X, Vlatkovic I, Babic A, Will T, Epstein I, Tushev G, Akbalik G, Wang M, Glock C, Quedenau C, Wang X, Hou J, Liu H, Sun W, Sambandan S, Chen T, Schuman EM, Chen W (2015) Neural circular RNAs are derived from synaptic genes and regulated by development and plasticity. Nature neuroscience 18:603-610.

Zhang J, Sun XY, Zhang LY (2015) MicroRNA-7/Shank3 axis involved in schizophrenia pathogenesis. Journal of clinical neuroscience : official journal of the Neurosurgical Society of Australasia 22:1254-1257.

1312 Zhang L, Chung SK, Chow BK (2014) The knockout of secretin in cerebellar Purkinje cells impairs mouse
1313 motor coordination and motor learning. Neuropsychopharmacology : official publication of the
1314 American College of Neuropsychopharmacology 39:1460-1468.
1315 Zhang S, Yang XN, Zang T, Luo J, Pan Z, Wang L, Liu H, Liu D, Li YQ, Zhang YD, Zhang H, Ding HL, Cao JL
1316 (2017) Astroglial MicroRNA-219-5p in the Ventral Tegmental Area Regulates Nociception in Rats.
1317 Anesthesiology 127:548-564.
1318 Zhang Y, Zhang XO, Chen T, Xiang JF, Yin QF, Xing YH, Zhu S, Yang L, Chen LL (2013) Circular intronic long
1319 noncoding RNAs. Molecular cell 51:792-806.
1320 Zhao X, Tang Z, Zhang H, Atianjoh FE, Zhao JY, Liang L, Wang W, Guan X, Kao SC, Tiwari V, Gao YJ, Hoffman
1321 PN, Cui H, Li M, Dong X, Tao YX (2013) A long noncoding RNA contributes to neuropathic pain by
1322 silencing Kcna2 in primary afferent neurons. Nature neuroscience 16:1024-1031.
1323 Zhao Y, Alexandrov PN, Jaber V, Lukiw WJ (2016) Deficiency in the Ubiquitin Conjugating Enzyme UBE2A in
1324 Alzheimer's Disease (AD) is Linked to Deficits in a Natural Circular miRNA-7 Sponge (circRNA;
1325 ciRS-7). Genes 7.
1326 Zheng Q, Bao C, Guo W, Li S, Chen J, Chen B, Luo Y, Lyu D, Li Y, Shi G, Liang L, Gu J, He X, Huang S (2016)
1327 Circular RNA profiling reveals an abundant circHIPK3 that regulates cell growth by sponging
1328 multiple miRNAs. Nature communications 7:11215.
1329 Zhou J, Xiong Q, Chen H, Yang C, Fan Y (2017) Identification of the Spinal Expression Profile of Non-coding
1330 RNAs Involved in Neuropathic Pain Following Spared Nerve Injury by Sequence Analysis. Frontiers
1331 in molecular neuroscience 10:91.
1332 Zhou Q, Yang L, Larson S, Basra S, Merwat S, Tan A, Croce C, Verne GN (2016) Decreased miR-199
1333 augments visceral pain in patients with IBS through translational upregulation of TRPV1. Gut
1334 65:797-805.

1335

1336

1337

1338

1339

1340

1341

1342

1343

Figure legends

Figure 1. Profiling of circRNAs and circRNA-Filip1l expression in mouse spinal cord. ***A,*** The expression profiling of differential circRNAs with 2 fold or more was generated from circRNA microarray. Spinal cord was collected 3 day after CFA- or Saline-injection. *n* = 3 per group. The number presents the identification of circRNA in Arraystar Mouse circRNA's Microarray. ***B,*** Four differential circRNAs were subjected to qRT-PCR verification. *n* = 4 per group; no significance versus the corresponding microarray groups by two-tailed paired Student's t test. ***C,*** The genomic loci of circRNA-Filip1l (ciR-Filip1l) is shown. The junction of circRNA-Filip1l was amplified by the use of back-to-back primers, and then sequenced by Sanger-Sequencing. Arrows represent divergent primers binding to the genome region of circRNA-Filip1l. ***D,*** Total RNAs were digested with RNase R followed by qRT-PCR detection of circRNA-Filip1l expression. Filip1l mRNA was detected as the RNase R-sensitive control. *n* = 4 per group; ***p<0.001 versus the corresponding mock groups by two-tailed paired Student's t test. ***E,*** Northern blot for circRNA-Filip1l in spinal cord of mice. SC, spinal cord; M, RNA marker. ***F,*** Distribution of circRNA-Filip1l in the nucleus and cytoplasma of spinal neuron cultured *in vitro*. Gapdh represents coding RNA control; Malat1, noncoding RNA control. Their levels were normalized to Gapdh. Spinal nucleus and cytoplasma RNA were collected respectively from 48 h cultured mouse spinal neurons *in vitro*.

1365 *n* = 4 per group. ***G,*** CircRNA-Filip1l FISH in the spinal neuron cultured *in vitro*.
1366 DAPI, nucleus staining dyes.
1367
1368 **Figure 2.** Chronic inflammatory pain induces the increase of spinal
1369 circRNA-Filip1l. ***A, B,*** Chronic inflammatory pain time-dependently led to the
1370 increase of circRNA-Filip1l in the ipsilateral (Ipsil) spinal dorsal horn (A), and to
1371 the slight increase of Ipsil spinal ventral horn (B) of mice. *n* = 5 per group; *p<0.05,
1372 **p<0.01 versus the corresponding Sal groups by two-tailed paired Student's t test.
1373 ***C, D,*** The injection of CFA did not change the expression of circRNA-Filip1l in the
1374 contralateral (Contral) spinal dorsal horn (C), and the Ipsil DRG (D) of mice. *n* = 5
1375 per group; no significance, versus the corresponding Sal groups by two-tailed
1376 paired Student's t test. ***E, F,*** Neuropathic pain induced by chronic constriction
1377 injury altered the content of circRNA-Filip1l day 3, 7 and 14 in spinal cord (C), but
1378 not in DRG (D) after surgery. *n* = 5 per group; *p<0.05 versus the related Sham
1379 groups by two-tailed paired Student's t test. ***G,*** Combined circRNA-Filip1l FISH
1380 (green) and NeuN (a neuronal marker, red) immunofluorescence staining in spinal
1381 cord day 3 after CFA or saline injections. Scale bar, 25 μm. ***H,*** The relative level of
1382 circRNA-Filip1l was analyzed by RT-PCR, respectively in spinal neurons, and
1383 astrocytes and microglial cells cultured *in vitro*. *n* = 6 per group; ***p<0.001 versus
1384 the related microglial groups by two-tailed paired Student's t test. ***I,***
1385 circRNA-Filip1l was increased after treatment with KCl (50mM) for 12 h in cultured

spinal neurons. *n* = 6 per group; **p<0.01 versus the related naïve groups by two-tailed paired Student's t test. ***J,*** Single cell real-time polymerase chain reaction (RT-PCR) shows the co-localization of circRNA-Filip1l with NeuN. Nos. 1−6 represents six different neurons; No. 7 (N) is a negative control. The spinal neurons were isolated from day 2 after CFA-injected mice with 4 weeks-old.

Figure 3. CircRNA-Filip1l contributes to nociceptive behavior. ***A,*** The infection of PLV-anti-Filip1l with GFP reporter in spinal cord of naïve mice day 3 after 2 consecutive days' intrathecal injection (day 5 after the first injection). NeuN, a neuron marker. Scale bar, 25 μm. ***B, C,*** Inhibition of circRNA-Filip1l alleviated the thermal hyperalgesia and mechanical allodynia after 2 consecutive days' intrathecal injections of anti-Filip1l (***B***) or PLV-anti-Filip1l (***C***) in CFA mice. *n* = 6 per group; *p<0.05, **p<0.01; two-way ANOVA (effect vs. group × time interaction) followed by post hoc Tukey test. Red arrow indicates CFA or saline injections; blue arrow, anti- Filip1l or Scr and PLV-anti-Filip1l or Vector injections. The anti-Filip1l sequence was antisense strand of full length of circRNA beginning from junction. ***D, E,*** Intrathecal injections of circRNA-Filip1l mimics (***D***) or Lenti-Filip1l (***E***) for 2 consecutive days increased the spinal circRNA-Filip1l content in naïve mice. *n* = 5 per group; p*<0.05, or **p<0.01; two-tailed paired Student's t test. ***F,*** The infection of Lenti-Filip1l with GFP reporter in spinal cord of naïve mice day 3 after 2 consecutive days' intrathecal injection. Scale bar, 25 μm.

G, H, Overexpression of circRNA-Filip1l induced the generation of pain-like behavior after 2 consecutive days' intrathecal injections of circRNA-Filip1l mimics (***G***) or Lenti-Filip1l (***H***). *n* = 6 per group; *p<0.05, **p<0.01; two-way ANOVA (effect vs. group × time interaction) followed by post hoc Tukey test. Blue arrow, circRNA-Filip1l mimics or Scr and Lenti-Filip1l or Lenti-vector injections.

Figure 4. MiRNA-1224 is an upstream negative regulator of circRNA-Filip1l. ***A,*** Schematic presentation of miRNA-1224 (miR-1224) binding to the fragment of pre-circRNA-Filip1l (pre-ciR-Filip1l). Underlined presents circRNA-Filip1l; blue, the reverse complementary of miR-1224 to pre-ciR-Filip1l. ***B,*** Distribution of miRNA-1224 in the nucleus and cytoplasma of spinal neuron cultured *in vitro*. *n* = 4 per group. Spinal nucleus and cytoplasma RNA were separated from spinal neurons cultured *in vitro* for 48 h. ***C,*** miRNA-1224 FISH in the spinal neuron cultured *in vitro*. ***D,*** CFA induced the time-dependent decrease of spinal miRNA-1224. *n* = 5 per group;*p<0.05, **p<0.01 versus the corresponding Sal groups by two-tailed paired Student's t test. ***E,*** Combining FISH of miRNA-1224 and IF of NeuN. Scale bar, 25 μm. ***F,*** The validation of miR-1224 negatively regulating circRNA-Filip1l by luciferase report assay *in vitro*. A fragment of pre-circRNA-Filip1l containing the bound region by miRNA-1224 was inserted into psiCHECK reporter vectors (psiCK-wt-pre-Filip1l). A mutation was generated via altering the sequence bound by miRNA-1224 as indicated (psiCK-mut-pre-Filip1l).

The wild and mutation reporters were co-transfected into the HEK293T with miRNA-1224 mimics or inhibitor or the scrambled. *n* = 4 per group; *p<0.05; two-way ANOVA (effect vs. plasmid × treated interaction) followed by post hoc Tukey test. ***G,*** Test for the binding capacity of miRNA-1224 to pre-circRNA-Filip1l *in vivo*. Spinal cord was harvested hour 24 after intrathecal injection of Bio-miRNA-1224 probes, fixed by formaldehyde, and the bound pre-circRNA-Filip1l was pull down by Dynabeads M-280 Streptavidin. *n* = 4 per group; *p<0.05 versus Sal group by two-tailed paired Student's t test. ***H,*** *In vitro* transfection of miRNA-1224 mimics or Lenti-1224 enhanced the miRNA-1224 level in HEK293T hour 48 after treatment. *n* = 4 per group; **p<0.01 versus the corresponding groups by two-tailed paired Student's t test. ***I,*** Intrathecal injections of miRNA-1224 mimics or Lenti-1224 for 2 consecutive days increased the miRNA-1224 content in spinal cord of naïve mice. *n* = 4 per group; p*<0.05, **p<0.01; one-way ANOVA (expression vs. the treated groups) followed by post hoc Tukey test. ***J, K,*** Intrathecal injections of miRNA-1224 mimics (***J***) or Lenti-1224 (***K***) for 2 consecutive days inhibited the expression of spinal circRNA-Filip1l, not changed the spinal pre-circRNA-Filip1l level day 2 after last injection in CFA mice. *n* = 5 per group; **p<0.01; one-way ANOVA (expression vs. the treated groups) followed by post hoc Tukey test. ***L, M,*** Intrathecal injections of miRNA-1224 inhibitor (***L***) or PLV-1224-sponge (***M***) for 2 consecutive days increased the expression of spinal circRNA-Filip1l, not changed the spinal

pre-circRNA-Filip1l level day 3 after last injection in naïve mice. *n* = 5 per group; **p<0.01 versus the corresponding control groups by two-tailed paired Student's t test.

Figure 5. MiRNA-1224 modulates the nociceptive behavior through the mediation of circRNA-Filip1l. ***A, B,*** Intrathecal injections of miRNA-1224 mimics (***A***) or Lenti-1224 (***B***) for 2 consecutive days reversed CFA-induced thermal hyperalgesia and mechanical allodynia during the maintenance period. *n* = 6 per group; *p<0.05, **p<0.01; two-way ANOVA (effect vs. group × time interaction) followed by post hoc Tukey test. Red arrow indicates CFA or Sal injections; blue arrow miRNA-1224 mimics or Scr and Lenti-1224 or Lenti-vector injections. ***C,*** Intrathecal pre-injection of Lenti-1224 for 2 consecutive days prevented the CFA-induced pain hypersensitivity during the development period. *n* = 6 per group; *p<0.05, **p<0.01; two-way ANOVA (effect vs. group × time interaction) followed by post hoc Tukey test. Blue arrow, Lenti-1224 or Lenti-vector injections; red arrow, CFA or Sal injections. ***D, E,*** Intrathecal injections of miRNA-1224 inhibitor (***D***) or PLV-1224 (***E***) for 2 consecutive days produced pain-like behavior in naïve mice. *n* = 6 per group; *p<0.05, **p<0.01; two-way ANOVA (effect vs. group × time interaction) followed by post hoc Tukey test. Black arrow, miRNA-1224 inhibitor or Scr and PLV-1224 or Vector injections. ***F,*** Intrathecal injection of anti-Filip1l significantly inhibited or prevented the pain hypersensitivity induced by PLV-1224

in naïve mice. *n* = 6 per group; *p<0.05; two-way ANOVA (effect vs. group × time interaction) followed by post hoc Tukey test. Red arrow, PLV-1224 injection; blue arrow, anti-Filip1l or Scr injection. ***G,*** Pre-treatment with anti-Filip1l significantly inhibited the pain hypersensitivity induced by miRNA-1224 inhibitor in naïve mice. *n* = 6 per group; *p<0.05; two-way ANOVA (effect vs. group × time interaction) followed by post hoc Tukey test. Red arrow, miRNA-1224 inhibitor injection; blue arrow, anti-Filip1l or Scr injections.

Figure 6. Ago2 mediates circRNA-Filip1l expression by cleavage of the pre-circRNA-Filip1l, and regulates the nociceptive behavior. ***A,*** Luciferase activities of reporter plasmid after co-transfection of miRNA-1224 mimics, Ago2 overexpression plasmid (Lenti-Ago2) or empty vector (Lenti-vector), and psiCK-mut-pre-Filip1l or psiCK-wt-pre-Filip1l into HEK293T. *n* = 4 per group; *p<0.05, **p<0.01; two-way ANOVA (effect vs. plasmid × treated interaction) followed by post hoc Tukey test. ***B,*** Co-immunoprecipitation of Ago2 and pre-circRNA-Filip1l or miRNA-1224. The pre-circRNA-Filip1l, miRNA-1224 and Ago2 complex was pulled down using anti-Ago2 antibody for spinal tissues 3 days after CFA injection. *n* = 4 per group; *p<0.05 versus the corresponding Sal groups by two-tailed paired Student's t test. ***C, D,*** The expression change of Ago2 protein after intrathecal injection of Lenti-Ago2 in naïve mice or CFA-induced pain mice (***C***), and knockdown of Ago2 with Ago2-siRNA and PLV-Ago2 in naïve mice (***D***). *n*

= 4 per group; *p<0.05; one-way ANOVA (expression vs. the treated groups) followed by post hoc Tukey test. ***E, F,*** Overexpression of Ago2 decreased the spinal circRNA-Filip1l content (***E***), but not pre-circRNA-Filip1l content (***F***) in CFA mice. Spinal cord was collected, respectively hour 3 after intrathecal injection of Ago2 protein, and day 2 after Lenti-Ago2 intrathecal injection. *n* = 5 per group; *p<0.05, **p<0.01; one-way ANOVA (expression vs. the treated groups) followed by post hoc Tukey test. ***G, H,*** Knockdown of Ago2 increased the spinal circRNA-Filip1l expression (***G***), not changed pre-circRNA-Filip1l level (***H***) day 2 after 2 consecutive day's Ago2-siRNA or PLV-Ago2 injections in naïve mice. *n* = 5 per group; *p<0.05, versus the corresponding control groups by two-tailed paired Student's t test. ***I, J,*** Overexpression of Ago2 alleviated the thermal hyperalgesia and mechanical allodynia induced by intrathecal injection of Ago2 (***I***) or Lenti-Ago2 for 2 consecutive days (***J***) in CFA mice. *n* = 6 per group; *p<0.05, **p<0.01; two-way ANOVA (effect vs. group × time interaction) followed by post hoc Tukey test. Red arrow, CFA injection; blue arrows, Ago2 or PBS (left) and Lenti-Ago2 or Lenti-vector (right) injections. ***K, L,*** Knockdown of Ago2 induced the thermal and mechanical hypersensitivity after 2 consecutive days' intrathecal injections of Ago2-siRNA (***K***) or PLV-Ago2 (***L***) in naïve mice. *n* = 6 per group; *p<0.05, **p<0.01; two-way ANOVA (effect vs. group × time interaction) followed by post hoc Tukey test. Black arrow, Ago2-siRNA or Scr and PLV-Ago2 or Vector injections. ***M,*** Inhibiting circRNA-Filip1l with anti-Filip1l prevented the thermal and

mechanical hypersensitivity induced by knockdown of Ago2 after 2 consecutive day's intrathecal injection of PLV-Ago2 in naïve mice. *n* = 6 per group; **p<0.01; two-way ANOVA (effect vs. group × time interaction) followed by post hoc Tukey test. ***N,*** Overexpression of miRNA-1224 did not change the pain hypersensitivity induced by knockdown of Ago2 with Ago2-siRNA for 2 consecutive days intrathecal injection in CFA mice. n = 6 per group; **p<0.01; two-way ANOVA (effect vs. group × time interaction) followed by post hoc Tukey test.

Figure 7. CircRNA-Filip1l regulates nociceptive response via positively targeting Ubr5. ***A,*** Schematic presentation of circRNA-Filip1l binding to near region of Ubr5 TSS. ***B,*** Validation of circRNA-Filip1l targeting Ubr5 by the use of luciferase reporter. The activities of the pGL6-Ubr5 encompassing TSS of Ubr5 region bound by circRNA-Filip1l were detected hour 24 after co-transfection of pGL5 or pGL6-Ubr5 with DNA3.1-Filip1l by firefly luciferase reporter assays in HEK293T cells. The pGL6 plasmid (empty vector) was used as the negative control; pGL6-Ubr5, plasmid with Ubr5 region bound by circRNA-Filip1l. DNA3.1-Filip1l, plasmid of circRNA-Filip1l overexpression. Values of luciferase activities for each plasmid were normalized for transfection efficiency by co-transfection with pRL-TK plasmid. *n* = 4 per group; **p<0.01, ***p<0.001; two-way ANOVA (effect vs. plasmid × treated interaction) followed by post hoc Tukey test. ***C,*** Single cell RT-PCR shows the co-expression of circRNA-Filip1l with miRNA-1224, Ago2, and

Ubr5 in the spinal neurons of mice. No. 7 is a negative control. ***D, E,*** Knockdown of Ubr5 reversed the increase of spinal Ubr5 protein 24h after intrathecal injection of Ubr5-siRNA (***D***) or day 2 after 2 consecutive day's intrathecal injection of PLV-Ubr5 (***E***) in CFA mice. *n* = 5 per group; *p<0.05, **p<0.01; one-way ANOVA (expression vs. the treated groups) followed by post hoc Tukey test. ***F,*** Intrathecal injection of Ubr5-siRNA for 2 consecutive days alleviated the hypersensitivity to thermal or mechanical stimulus in CFA mice. Red arrow, CFA or Sal injections; Blue arrows, Ubr5-siRNA or Scr injections. *n* = 6 per group; *p<0.05, **p<0.01; two-way ANOVA (effect vs. group × time interaction) followed by post hoc Tukey test. ***G,*** Intrathecal injection of PLV-Ubr5 for 2 consecutive days inhibited the pain sensitivity in CFA mice. Red arrow, CFA or Sal injections; Blue arrows, PLV-Ubr5 or Vector injections. *n* = 6 per group; *p<0.05, **p<0.01; two-way ANOVA (effect vs. group × time interaction) followed by post hoc Tukey test. ***H,*** Inhibiting circRNA-Filip1l via intrathecal injection of anti-Filip1l for 2 consecutive days reversed the increase of Ubr5 protein in CFA mice. *n* = 5 per group; *p<0.05; one-way ANOVA (expression vs. the treated groups) followed by post hoc Tukey test. ***I, J,*** Up-regulating circRNA-Filip1l via intrathecal injections of circRNA-Filip1l mimics (***I***) or Lenti-Filip1l (***J***) for 2 consecutive days increased the expression of Ubr5 protein in naïve mice. *n* = 5 per group; *p<0.05, **p<0.01; one-way ANOVA (expression vs. the treated groups) followed by post hoc Tukey test. ***K,*** Intrathecal pre-injection of PLV-Ubr5 for 2 consecutive days prevented the thermal

hyperalgesia and mechanical allodynia induced by circRNA-Filip1l during the development period. *n* = 6 per group; *p<0.05, **p<0.01; two-way ANOVA (effect vs. group × time interaction) followed by post hoc Tukey test. Blue arrow, PLV-Ubr5 or Vector injections; Red arrow, circRNA-Filip1l mimics or Scr injections. ***L,*** Intrathecal post-injection of Ubr5- siRNA for 2 consecutive days inhibited the pain hypersensitivity induced by Lenti-Filip1l during the development period. *n* = 6 per group; *p<0.05, **p<0.01; two-way ANOVA (effect vs. group × time interaction) followed by post hoc Tukey test. Red arrow, Lenti-Filip1l or Lenti-vector injections. Blue arrow, Ubr5-siRNA or Scr injections.

Figure 8. The schematic of miRNA-1224 splicing circRNA-Filip1l in an Ago2-dependent manner regulates chronic inflammatory pain via targeting Ubr5.

Table 1.

Test was peformed 48 h after intrathecally injection of mimics, anti-RNA and Scr or 72 h after intrathecal injection of Lentivirus for 2 consecutive days in mice. No significance; one-way ANOVA (response time vs. the treated groups) followed by post hoc Tukey test. SEM given in parentheses. *n* = 5 mice per group; five trials.

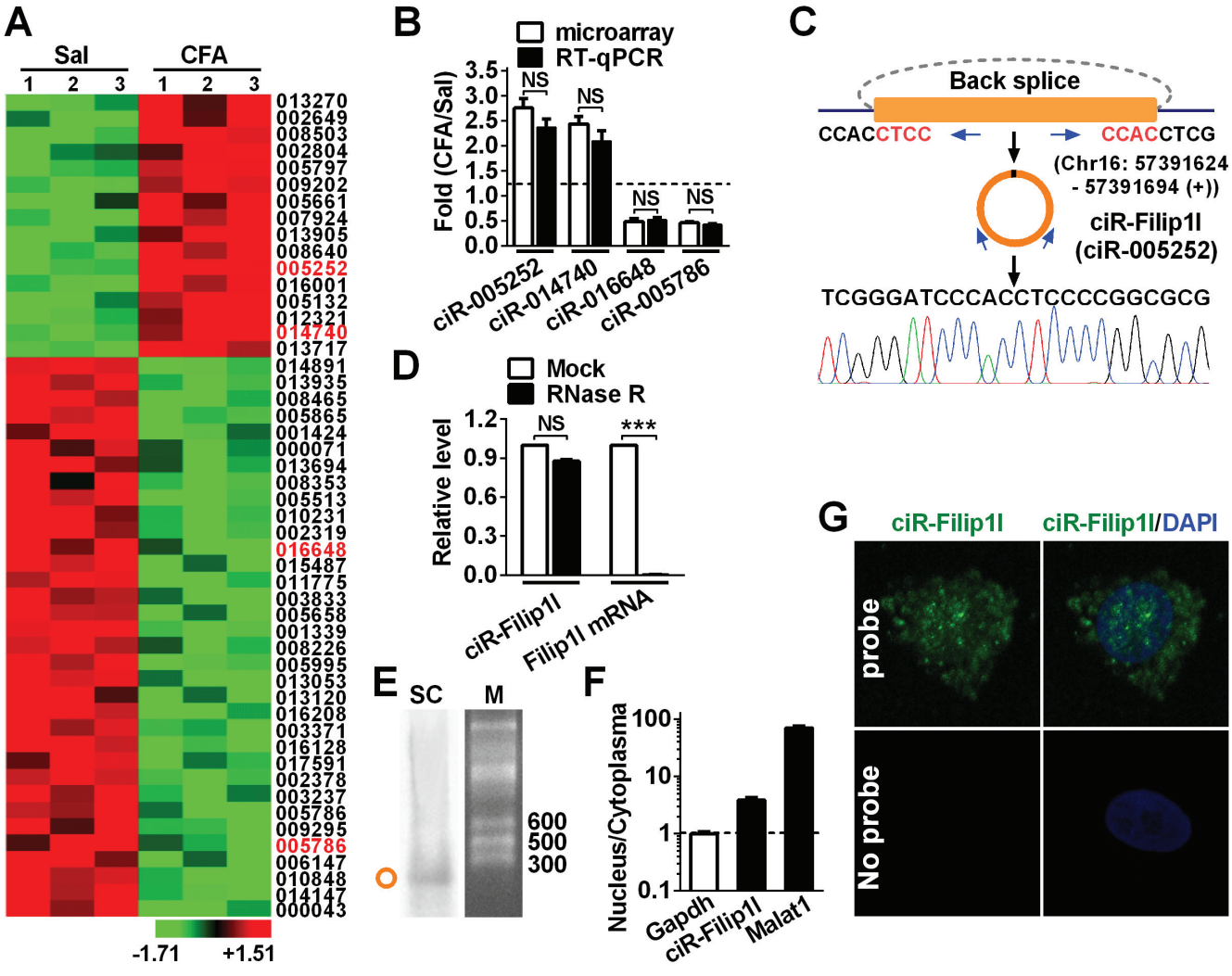

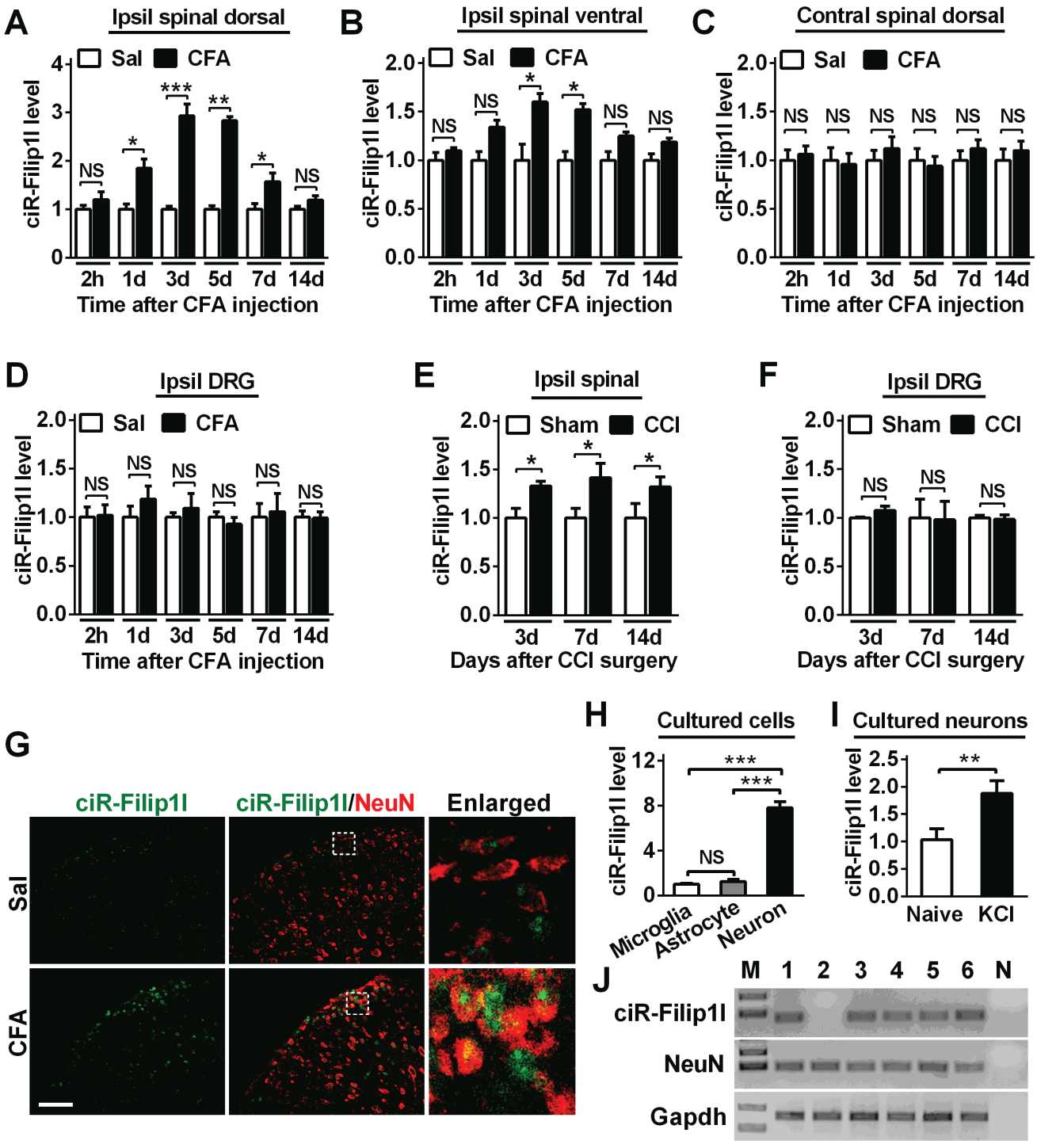

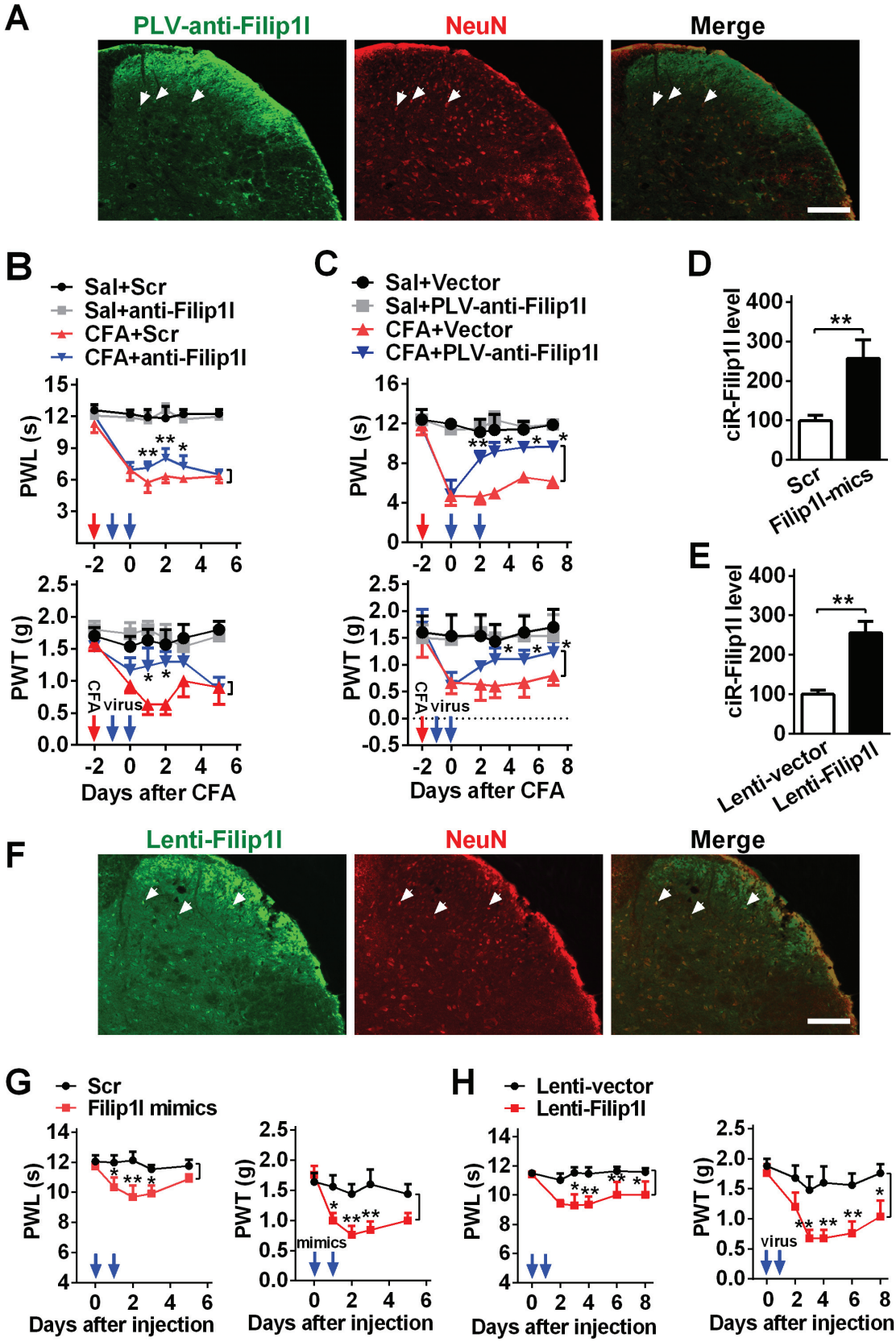

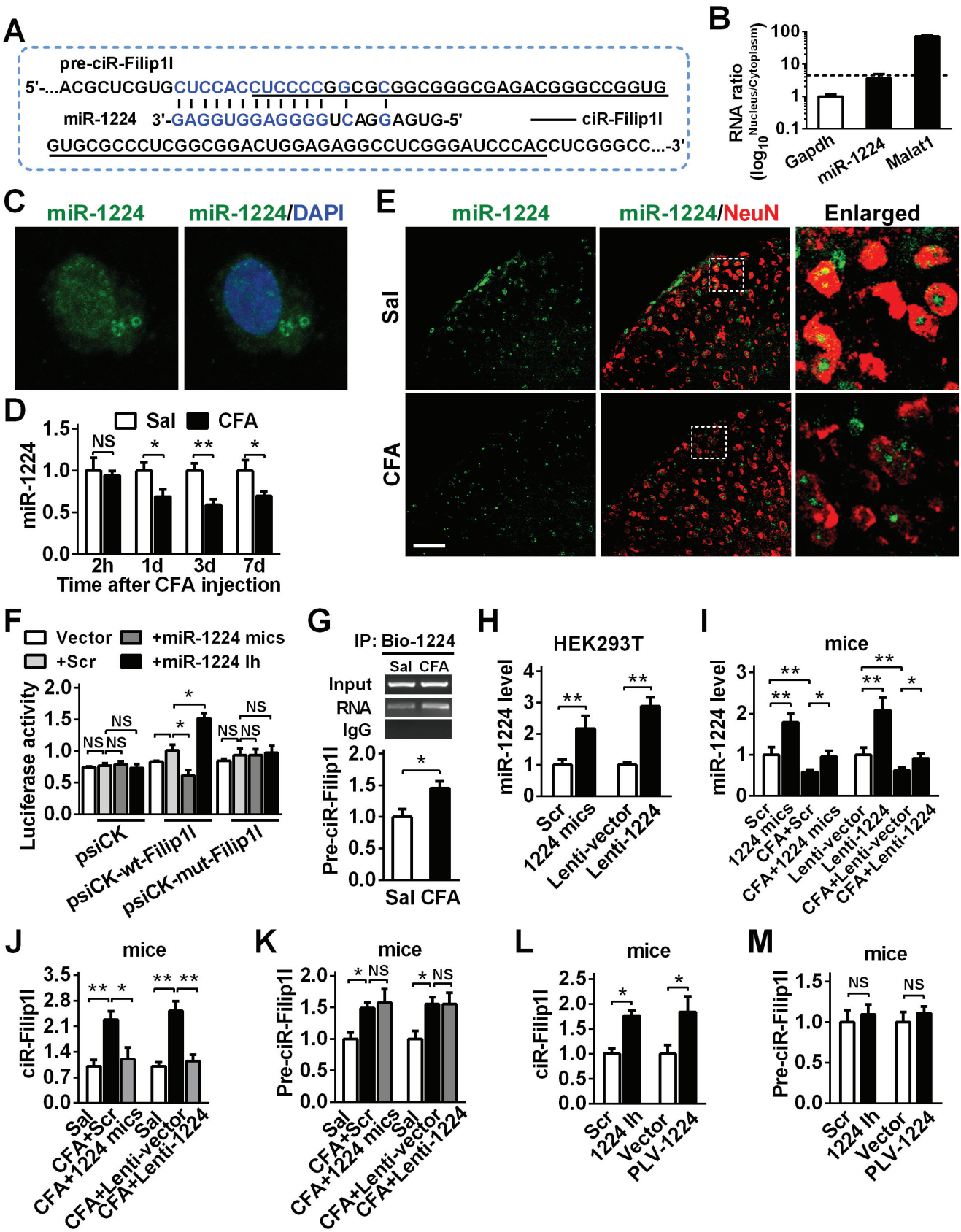

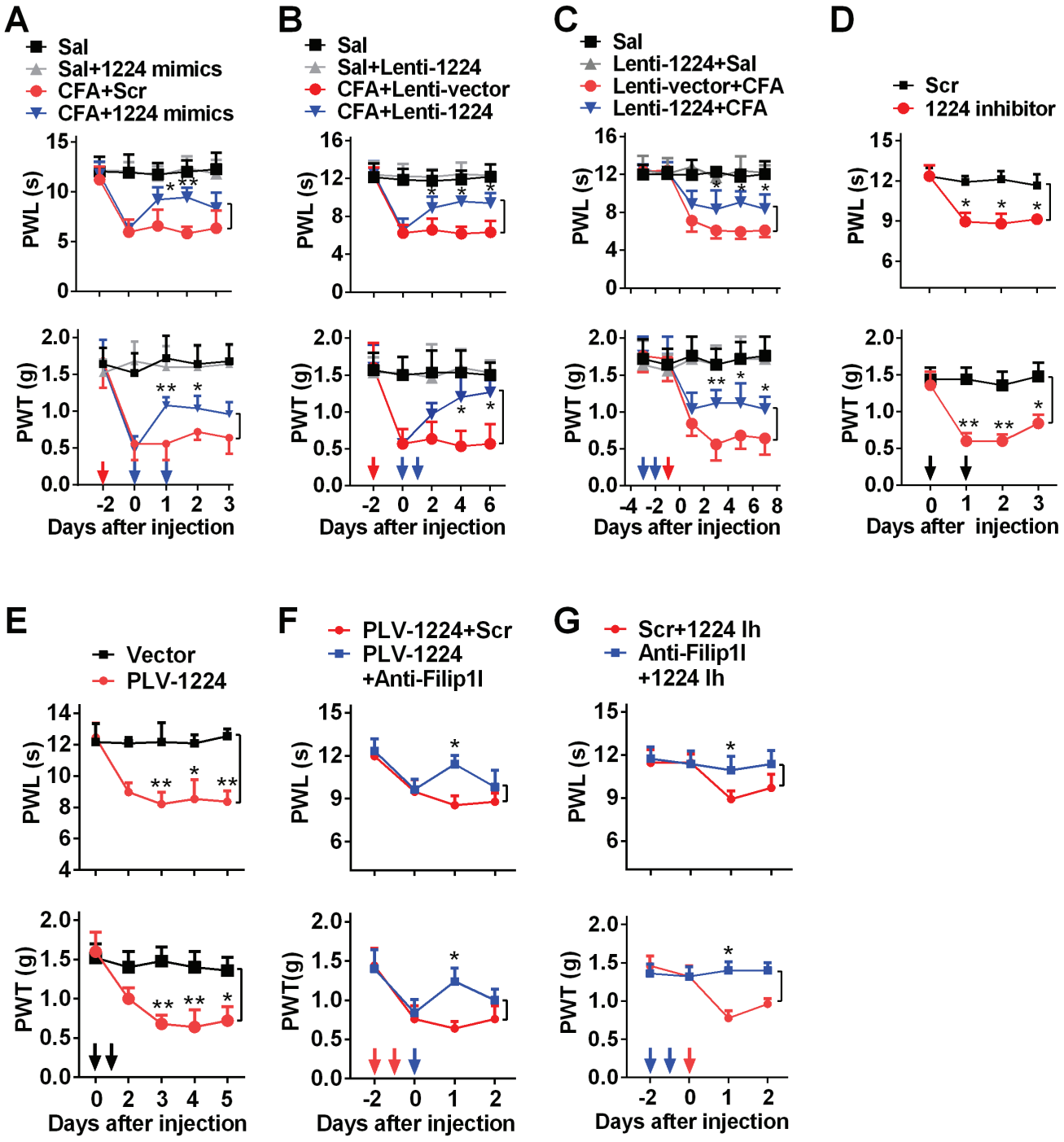

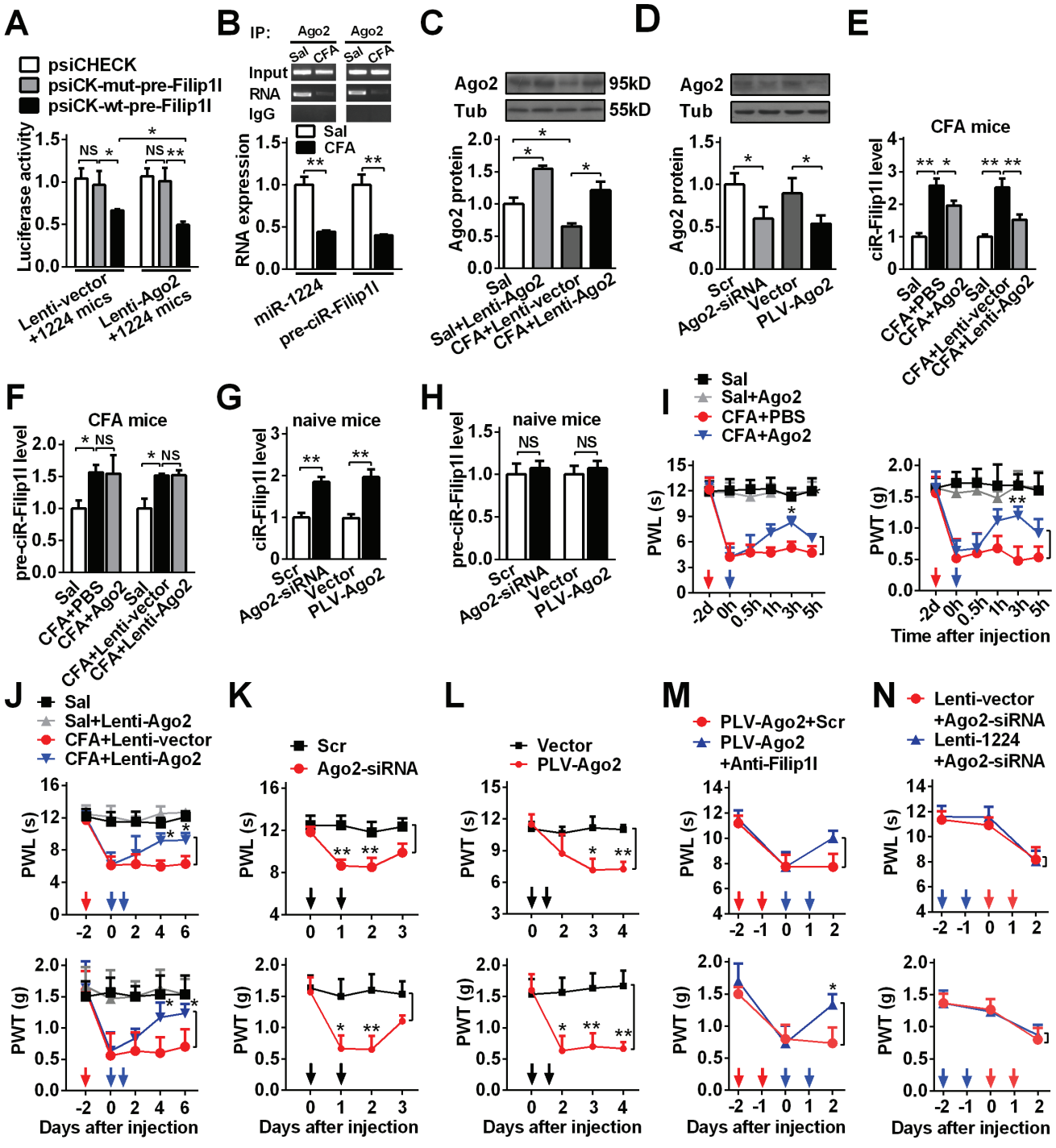

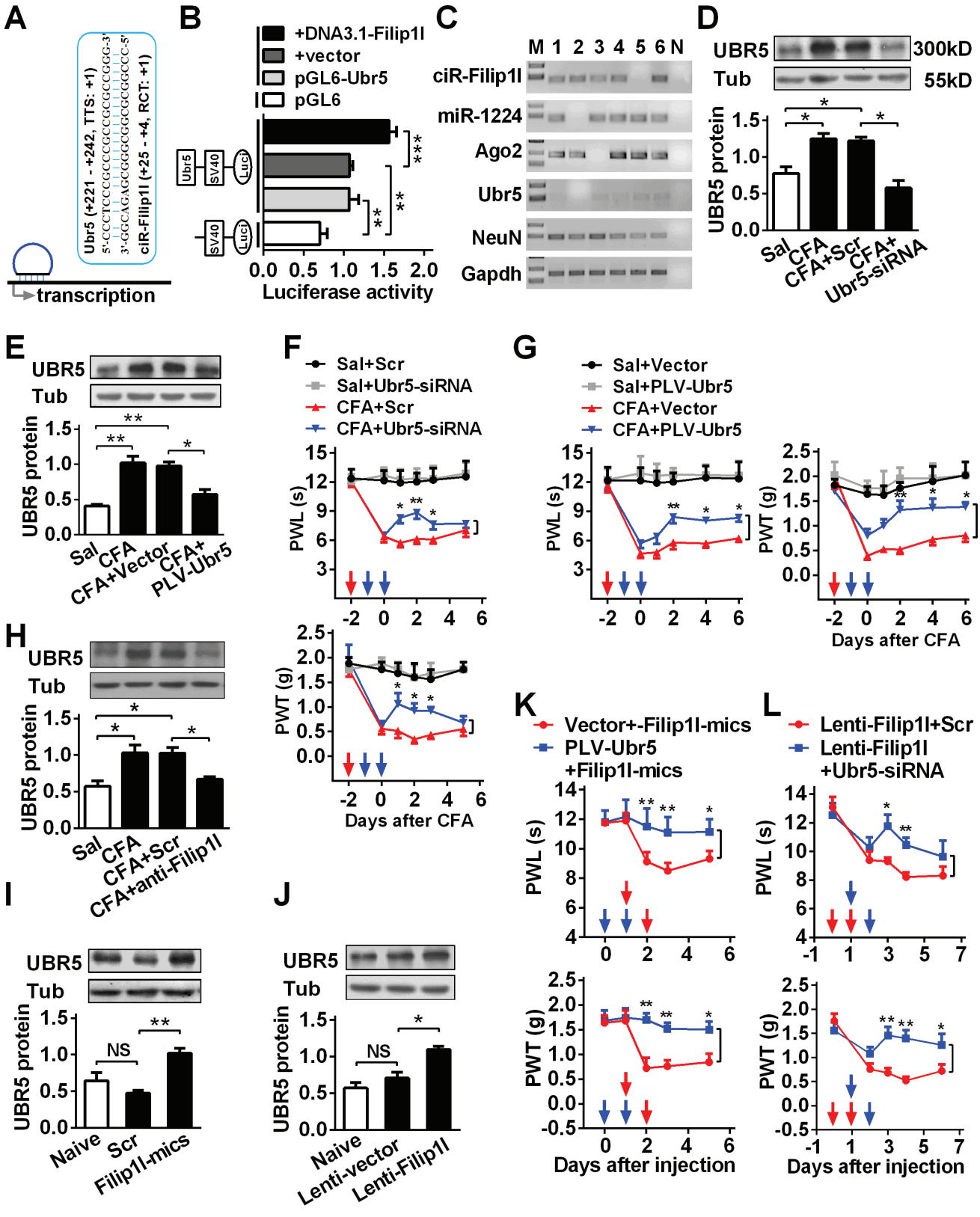

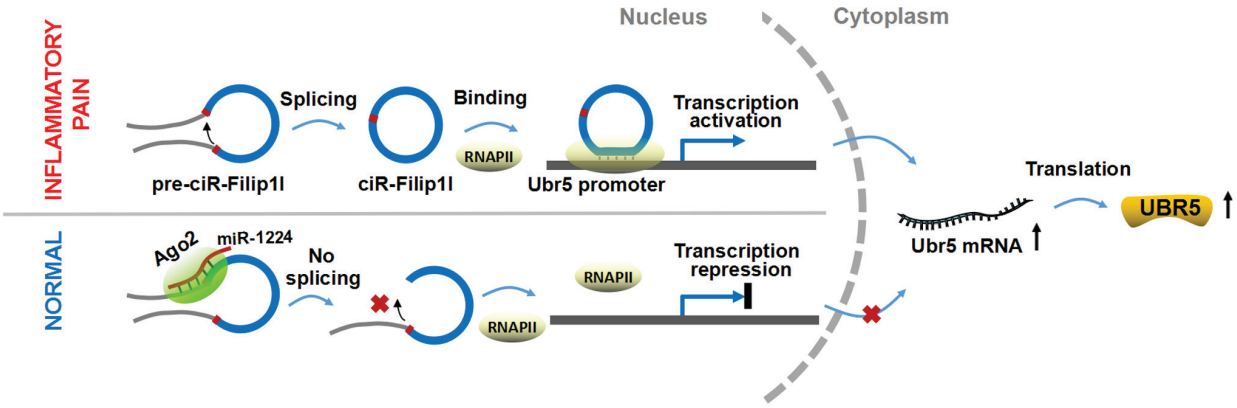

Table 1. Mean changes in locomotor function.

Treatment groups	Locomotor function test		
	Placing	Grasping	Righting
Saline (5 μl)	5(0)	5(0)	5(0)
Negative control siRNA (Scr)	5(0)	5(0)	5(0)
PLVTHM empty vector (Vector)	5(0)	5(0)	5(0)
Pwpxl empty vector (Lenti-vector)	5(0)	5(0)	5(0)
Sal + Scr	5(0)	5(0)	5(0)
Sal + anti-Filip1l	5(0)	5(0)	5(0)
CFA + Scr	5(0)	5(0)	5(0)
CFA + anti-Filip1l	5(0)	5(0)	5(0)
Sal + Vector	5(0)	5(0)	5(0)
Sal + PLV-anti-Filip1l	5(0)	5(0)	5(0)
CFA + Vector	5(0)	5(0)	5(0)
CFA + PLV-anti-Filip1l	5(0)	5(0)	5(0)
circRNA-Filip1l mimics	5(0)	5(0)	5(0)
Lenti-circRNA-Filip1l	5(0)	5(0)	5(0)
Sal + miRNA-1224 mimics	5(0)	5(0)	5(0)
CFA + miRNA-1224 mimics	5(0)	5(0)	5(0)
Sal + Lenti-miRNA-1224	5(0)	5(0)	5(0)
CFA + Lenti-miRNA-1224	5(0)	5(0)	5(0)
miRNA-1224 inhibitor	5(0)	5(0)	5(0)
PLV-miRNA-1224	5(0)	5(0)	5(0)